# Arctic soil development under changing climate conditions

Maud A.J. van Soest [a,b,*], N.John Anderson [a], Joanna E. Bullard [a]

[a] Geography and Environment, Loughborough University, Loughborough LE11 3TU, United Kingdom
[b] UK Centre for Ecology & Hydrology, Environment Centre Wales, Deiniol Road, Bangor LL57 2UW, United Kingdom

A B S T R A C T

As global temperatures rise, soil dynamics in areas affected by changing snow and permafrost are increasingly important due to their impact on carbon release and ecosystem functionality. This study examines soil development and variability in Kangerlussuaq, southwest Greenland, from the ice margin to inland areas, assessing how soil characteristics evolve with time since glacial retreat and across different spatial scales. The findings highlight the interaction between geomorphic and pedogenic processes, with soils influenced by glacial deposition, aeolian inputs, and topography. The most common soil groups include Regosols, Cambisols, Cryosols and Histosols. Soil depths range from shallow layers constrained by bedrock or permafrost to more developed profiles exceeding 80 cm, with an average depth of 24–40 cm. Buried organic layers and paleosols reflect the area's aeolian history and could partly explain the highly variable distribution of soil organic carbon showing weak or inconsistent correlations with slope and aspect, although organic carbon content was higher on cooler wetter north-facing slopes. Future permafrost thaw will disproportionately impact ice-rich soils in waterlogged and north-facing areas, releasing stored carbon and potentially accelerating climate feedback loops. In contrast, south-facing slopes with seasonal thaw will experience minimal structural change. This research established a detailed baseline for monitoring changes in soil properties and carbon dynamics over time, particularly as warming continues to affect Arctic environments.

## 1. Introduction

### 1.1. Arctic soils in a warming climate

In cold and dry environments, soil development (soil evolution over time) progresses slowly due to low rates of weathering and biological turnover (Hodkinson et al., 2003; Meier et al., 2019) which, in combination with permafrost formation, has led to the accumulation of vast amounts of carbon (C) stored in cold region soils (Tarnocai et al., 2009; Hugelius et al., 2013; Schuur et al., 2015). Soils in the Arctic should occupy a central role in regional and global ecosystem models linking and providing feedback responses to water cycles, atmospheric interactions, and vegetation growth (Minasny et al., 2015). This is particularly relevant in a warming world, as shifts in soil properties in areas where snow and permafrost dynamics are changing can have a cascading effect on broader ecosystem functionality, influencing carbon release, nutrient availability, and biodiversity (Temme et al., 2016; Vonk et al., 2019; Bosson et al., 2023).

Climate warming is changing the role of Arctic soil development within the biosphere (Doetterl et al., 2022). Permafrost thaw could accelerate decomposition and hence C mineralisation or it could enhance vegetation growth and increase C inputs to the soil (Schaphoff et al., 2013; Bowen et al., 2020). The exponential nature of microbial decomposition and $CO_2$ and $CH_4$ release over time means that the initial decades after permafrost thaw will be the most important for greenhouse gas release for any particular unit of thawed soil and it is estimated that 5–15 % of the terrestrial permafrost C stock maybe released during this century (Schuur et al., 2015). Temperature-induced increase in soil respiration creates a positive feedback loop between climate warming and C loss from soils to the atmosphere (Phillips et al., 2019). Permafrost degradation and subsequent erosion could potentially expose and release large amounts of C currently stored in frozen and unfrozen soils, thereby accelerating feedback to climate warming, but the increase in vegetation productivity and shrub expansion, in some cases linked to permafrost degradation, could instead stabilize soil particles, reduce summer heat flux, and promote permafrost development (Tape et al., 2011).

## 1.2. Time since deglaciation and spatial variation in soil C

Climate warming is expected to result in the loss of 22 ± 8 % to 51 ± 15 % of the glaciated areas on Earth, and the associated change in albedo and potential release of stored C may contribute to further temperature increase. Conversely, the development of post glacial ecosystems may contribute to C uptake through evolving biogeochemical processes such as pedogenesis and plant succession (Eichel et al., 2013; Bosson et al., 2023). The retreat of glaciers has exposed new land surfaces, creating a unique opportunity to study early soil development under harsh Arctic conditions. Time since deglaciation is considered a proxy for the start of soil formation (how soils originate and evolve). Soil characteristics related to the degree of soil development, influence the turnover rate of organic matter (OM) and mobility of C within the soil (Henkner et al., 2016). More specifically, differences in soil development may lead to varying SOC dynamics and these dynamics are likely to change over time when soils further develop (Lawrence et al., 2021). Furthermore, both the input of C from litter and the uptake of C by plants highly depend on the type of vegetation cover (Hobbie et al., 2002) and vegetation succession also progresses with time.

Disturbances such as erosion or increased nutrient supply through aeolian deposition Fowler et al., 2018; van Soest et al., 2022) can respectively delay or accelerate soil development, leading to noticeable variations in soil characteristics even on small spatial scales (Wojcik et al., 2021). Hence, the biogeochemical response to permafrost degradation can be site specific (Tank et al., 2020). Terrestrial ecosystems in general are highly sensitive to e.g. soil texture, and ecosystem response to climate warming at the landscape scale will vary nonlinearly in response to local soil conditions (Rosenbloom et al., 2001). The role of soil formation and development will therefore be key to understanding the complex feedback loops in Arctic (Doetterl et al., 2022).

## 1.3. Geomorphic and pedogenic soil forming processes

Soil formation is a complex and continuous process shaped by the interplay of multiple factors that vary across space and time (Jenny, 1941). Understanding soil development and identifying the most dominant soil-forming factors is often challenging. Each soil unit (pedon) within a specific landscape is simultaneously influenced by geomorphic and pedogenic processes (van der Meij et al., 2016). Geomorphic processes, which operate laterally, primarily affect the top layers of the soil profile by adding or removing particles across the soil surface. These processes include aeolian (wind-driven), fluvial (water-driven) or gravitational movements, all shaped by landscape topography. Pedogenic processes, on the other hand, are vertical and involve the movement or transformation of materials between soil layers through mechanisms such as weathering, percolation, leaching, biological mixing and turnover, as well as frost action in cold climates. Crucially, geomorphic and pedogenic processes are not mutually exclusive. Changes in geomorphology, such as shifts in topography or erosion patterns, directly influence pedogenic processes by altering the conditions under which soil layers develop.

In pedogenic processes, it is suggested that at local scales in stable locations of the same age, subtle differences in soil-forming factors such as parent material, climate, biota, and topography can lead to variations in soil development (Temme and Lange, 2014). For instance, slope aspect significantly affects soil development by influencing the amount of solar radiation received. In the Arctic, north-facing slopes, which receive less sunlight, can develop soils at very different rates compared to south-facing slopes that are more exposed to solar radiation (Egli et al., 2006). Other topographic features, such as variations in slope gradient, can enhance soil moisture levels or create differences in microclimates through shading, further influencing soil formation rates (Lev and King, 1999). To better understand how geomorphic processes affect soil development at the catchment level, a toposequence or soil catena approach is highly suitable. Introduced by Milne (1935), the soil catena concept refers to a sequence of soils connected by topography, with soils occupying different positions along a slope or landscape. This approach emphasizes that soil formation cannot be fully understood in isolation but must be considered in relation to other soils in the catena, as materials are exchanged between them by geomorphic processes such as erosion, deposition and runoff (Sommer and Schlichting, 1997).

## 1.4. Aeolian deposition and sediment

Soil depth depends on mass input and loss; including all mass and volume changes due to the mineral transformation of the parent material into soil (by chemical and physical weathering processes), the lowering of the bedrock/parent material-soil boundary, and atmospheric deposition and net organic matter input (Egli et al., 2018). A clear distinction should be made between soil and sediment. In the geomorphic definition, soil is the mobile portion of the weathering profile, as a material that no longer retains the fabric of the parent rock or sediment (Amundson et al., 2015). Bock et al. (2018) argue that in most cases the weathered part of the parent material on which soils develop is considerably thicker than the soil itself.

In areas of low rainfall or poor hydrological connectivity, amounts and timing of aeolian deposition, in combination with other soil forming factors, shows to cause spatial differences in the development of soils (Drohan et al. 2020). Varying aeolian influence on soils leads to the development of a range of soil profiles over time due to the interaction between aeolian particle transport and topography (Mason et al., 1999; Muhs, 2013). Coarser particles travel for example shorter distances and are expected to be deposited immediately downwind of a high point, whereas finer particles are more widely distributed (Goossens, 1996; Goossens, 2006).

The aim of this study is to investigate the interactions between soil development, time since exposure following ice retreat, local and regional topography, and aeolian dust inputs. and the study site is an ice-free area of southwest Greenland. It is assumed that the soils have been shaped by three initial processes: the deposition of sediments left behind after glacial retreat or introduced through aeolian processes, physical and chemical weathering and thirdly, translocation through erosion and sedimentation. These processes, in conjunction with the five key soil-forming factors – parent material, climate, organisms, topography and time (Jenny, 1941) – are expected to result in a heterogeneous geomorphology with diverse soil characteristics across the region. Five sites were selected at varying distances from the ice margin with the aim to provide a comprehensive understanding of Arctic soil variability in the region, shedding light on how soil development may respond to ongoing climatic and geomorphic changes in the region.

## 2. Methods

### 2.1. Study area

The study area is located near Kangerlussuaq in southwest Greenland (Fig. 1). Ice margin retreat, at an averagee rate of 15–20 m yr$^{-1}$ (Winsor et al., 2015), triggered a transition from a marine-terminating to a terrestrial based ice sheet with interrupted periods of further deglaciation marked by the deposition of the Taserqat, Sarfartôq-Avatdleq, Fjord and Umîvît-Keglen moraine systems between ~ 9.3 and ~ 7.3 ka BP (Young and Briner, 2015). The Ørkendalen moraines at the current ice margin are dated to ~ 6.8 ka and ~ 7.0 ka BP (van Tatenhove et al., 1996). During the warmer mid-Holocene, the ice sheet covered a smaller area than its current extent. Willemse et al. (2003) suggested that the Greenland Ice Sheet (GrIS) retreated > 15 km inland of its current position between ~ 3.4 and ~ 0.5cal ka BP based on aeolian activity in the region, but the exact minimum extent is poorly understood. Young and Briner (2015) tentatively estimated a retreat of ~ 10 km after 4.2cal ka BP and conclude that the ice margin re-advanced and likely has remained within ~ 1 km of its current position since ~ 1.8cal ka BP.
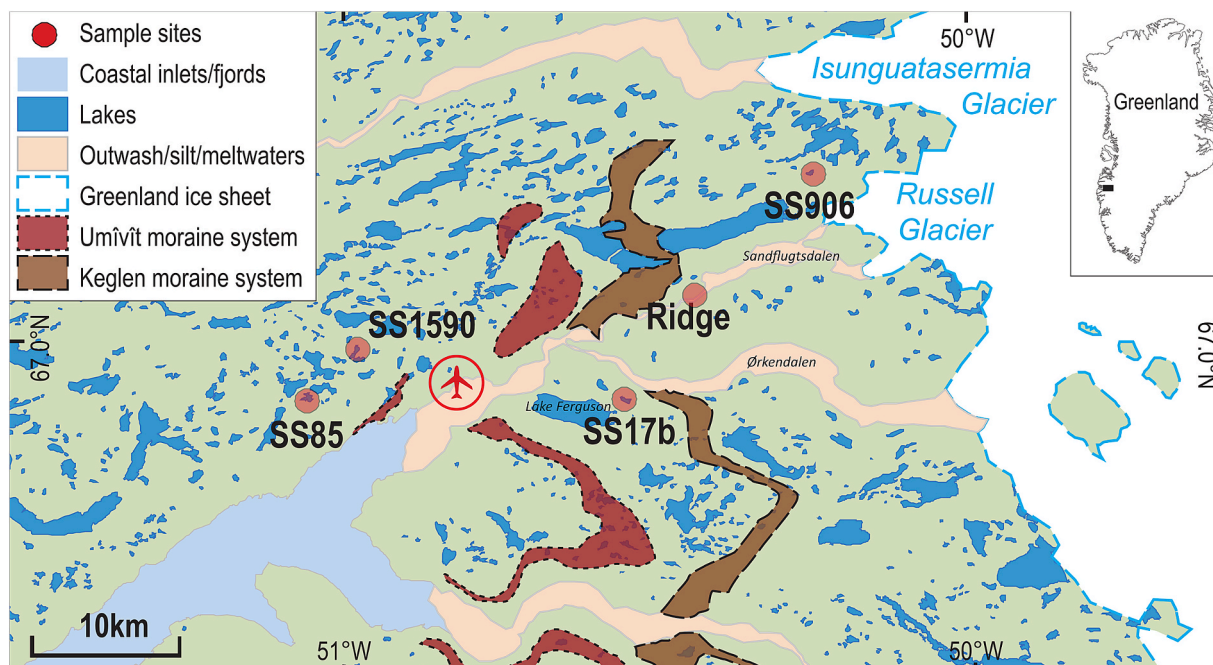
**Fig. 1.** Location of the study sites in proximity to the GrIS and moraines. Kangerlussauq airport is indicated with an icon. Position of dated moraines is taken from Tatenhove et al., (1996).

The bedrock geology is predominantly ancient granodiorite gneiss with occasional ultra-basic intrusions. The glacial floodplains and Kangerlussuaq Fjord form the source of regionally deposited loess (Eisner et al., 1995). The suggested timing of soil formation ranges from 4.5cal ka BP (van Tatenhove et al., 1996), to 3.4cal ka BP (Willemse et al., 2003; Dijkmans and Törnqvist, 1991) to 1.6/1.5cal ka BP (Ozols and Brol, 2005). Although there is variation in the suggested onset of soil formation, all studies highlight a strong connection to ice sheet dynamics. In this study, it was assumed that the dated moraine systems and phased ice retreat could be used as an indication for the start of soil formation in the Kangerlussuaq region. This gradient in time since deglaciation not only influences the start of soil development and vegetational succession but also incorporates changes in climatic conditions and aeolian activity.

The mean annual air temperature is –5.6 °C, characteristic of a continental arid interior with warm summers where temperatures can reach 16C in early July (Anderson et al., 2012). Annual precipitation is on average $< 200$ mm yr$^{-1}$ with most rainfall falling in the late summer. The thickness of the permafrost is estimated between 100 and 150 m (Van Tatenhove and Olesen, 1994) with an active layer depth between 0.3 and 2.0 m in open terrain during the summer (Petrone et al., 2016).

Soils have a texture of loam with coarse silt and processes in the surface layer are mainly driven by vegetation and aeolian silt deposition (Ozols and Broll, 2005). Henkner et al. (2016) classified soils in the Umimmalissuaq valley, about 30 km southeast of Kangerlussuaq, as haplic Regosols and Cryosols. Paleosols developed in the aeolian sediments around Kangerlussuaq indicate an interruption or decrease in aeolian activity and can be taken as proxies for stable conditions (Müller et al., 2016). Retreating glaciers left a mixture of fine sediments and rocks behind (Anderson, 2005), and these are clearly visible in the study area at the surface on higher ground and steeper south facing slopes. The fine sediment layer can reach substantial depths under continuous aeolian inputs in stable locations.

Extensive aeolian deposits can be observed on vegetation and snowbanks at the end of the winter and can form visible physical soil crusts, particularly where soils are thinner, due to the incorporation of dust into the organic matrix (Böcher 1949, Willemse et al., 2003). Most of the aeolian dust in Kangerlussuaq has a local origin (van Soest et al., 2022). Dominant dust carrying winds travel both up-valley (towards the ice) and down-valley (away from ice) (Bullard et al., 2023; Bullard and Mockford, 2018). Down-valley (katabatic) winds are typically stronger/ higher velocity and can transport coarser particles. Up-valley (sea breeze or regional) winds are weaker but can still transport fine sediments and mostly occur during the summer months (Bullard and Mockford, 2018).

Vegetation cover is extremely heterogeneous and ground cover can vary significantly across scales of a few meters (Anderson, 2020). The most common vegetation is dwarf-shrub tundra with *Betula nana, Salix glauca, Vaccinium* spp.*, Empetrum nigrum*, and various herbs and grasses as co-dominants (Anderson, 2020). Unvegetated ground is more common at higher altitudes and on south-facing slopes. Biological soil crusts take roughly 200 years to fully develop within these bare areas and play an important role in nitrogen cycling and soil stabilisation (Heindel et al., 2015), as observed in deglaciated areas elsewhere (Eichel et al., 2013; Eichel et al., 2016).

### 2.2. Site selection

Five sites (Fig. 1; Fig. 2; Table 1) were selected based on accessibility and distance to the ice. Four sites focus on soils developed on the catchment slopes around small lakes (prefix SS) which have previously been studied by e.g., Anderson et al. (2012); Saros et al. (2019). The numerical labels used elsewhere have been retained here for consistency and allow data relating to the catchments from this study to be associated with previous work. The fifth site (Ridge) is the head of a ridge located in Sandflugtsdalen, which is one of the main dust sources.

SS85 is located furthest (37.4 km) from the ice sheet. The site surrounds a clover-leaf shaped lake located at an altitude of about 190 m a. s.l. South-facing slopes are covered with *Salix glauca*, grasses and bare patches. The north facing slopes are hummocky and covered with mixed vegetation and *Betula nana*.

SS1590 (33.4 km) is a long and thin east–west orientated catchment dominated by north-west and south-east facing slopes with varying steepness and curvature. Low-lying flat areas and more gentle slopes are covered in grasses. Steep north-facing slopes have shallow organic layers covered with moss and are overlaying permafrost. Steep south-facing slopes are sparsely vegetated.

**Fig. 2.** Overview pictures looking down from the north facing slope at SS85, the southeast facing slope at SS1590, the north facing slope at SS17b, the north facing slope at SS906 and towards the GrIS in the east at the Ridge.

**Table 1**
Site characteristics with the catchment boundaries being based on the highest surrounding contour lines and field observations.

| Catchment | SS85 | SS1590 | SS17b | SS906 |
|---|---|---|---|---|
| Latitude N | 67º0'9.522″ | 67º0'52.5708″ | 66º59'16.8216″ | 67º6'55.9044″ |
| Longitude W | 51º0'39.114″ | 50º58'50.7396″ | 50º33'0.3672″ | 50º15'58.1004″ |
| Total area (m$^2$) | 1,307,775 | 1,085,212 | 626,705 | 502,740 |
| Lake (m$^2$) | 267,806 | 232,263 | 123,779 | 92,357 |
| Terrestrial (m$^2$) | 1,039,969 | 852,949 | 502,926 | 410,383 |
| Distance from the Ice Sheet (km) | 37.4 | 33.4 | 18.5 | 1.8 |
| Number of sampling points | 35 | 45 | 35 | 40 |
| pH | 6.7 ± 0.27 | 6.6 ± 0.22 | 6.7 ± 0.21 | 6.6 ± 0.30 |
| Wetness | 4.7 ± 2.43 | 5.1 ± 2.33 | 4.7 ± 2.40 | 6.3 ± 1.89 |
| LOI (%) | 5.25 ± 2.64 | 3.74 ± 2.14 | 4.00 ± 1.95 | 2.91 ± 1.31 |
| Fine earth fraction (%) | 0.95 ± 0.07 | 0.93 ± 0.08 | 0.97 ± 0.05 | 0.98 ± 0.04 |
| Depth of active layer (cm) | 24 ± 2.9 | 24 ± 2.9 | 33 ± 3.8 | 40 ± 2.9 |
| Based on number of sampling points at: | | | | |
| - Bedrock | 9 | 11 | 8 | 9 |
| - Permafrost | 5 | 5 | 3 | 2 |
| - Full depth not reached | 1 | – | 2 | 2 |

SS17b (18.5 km) is located south and downwind of Ørkendalen. The Ørkendalen outwash plain is at an altitude of 90 m a.s.l. but bounded by steep slopes of bedrock and the higher elevated lake catchment (235 m a.s.l.) might be sheltered from the wind blowing off the sandur. Slopes surrounding the lake are steep with an average angle of 25 degrees. Some boulders reach up to about 1.5 m in height and deeper soil profiles have developed behind these obstacles. West of the lake is a ridge separating SS17b from the lower elevated lake Ferguson valley. The ridge crest is bare, and the slope covered with a mixture of predominantly *Betula nana* and some *Salix glauca*. A small rock conglomerate coming from the southeast facing rockface borders the north of the lake. The flat area on the east side of the lake is covered with grasses. A different type of bedrock (Amphibolite instead of the dominant Orthogneiss) (Wallroth et al., 2010) might have implications for weathering rates and elemental composition of the parent material at this site.

The Ridge (5.6 km) is characterised by windblown deposits on a hill to the west (downstream) of the widest part of the Sandflugtsdalen outwash plain with the meltwater river incising on the south facing slope. Several small ridges can be distinguished over an increasing elevation of 125–250 m a.s.l. Vegetation changes with elevation and distance from the floodplain but is also visibly influenced by aspect and small-scale topography. The lowest part of the ridge is covered with mosses and mixed vegetation. The wetter convex parts higher up the slope contain mainly grasses. Concave crests are bare. Slopes facing slightly northwards are covered with *Betula nana*, whereas the more south facing slopes are covered with *Salix glauca* and grasses interspersed with bedrock and bare patches.

SS906 (1.8 km) is located closest to the ice sheet at an average elevation of 400 m a.s.l. and is one of the few lakes in the area with a water inlet through a bog area at the east. A terraced lake bank forms a ring around the lake of very organic soils covered with mosses and short vegetation. A steep bare rockface forms the north boundary of the catchment with aeolian deposits at the foot slope held together by grasses and occasionally *Salix glauca*. Other slopes are vegetated with a mixture of *Salix glauca* and *Betula nana*, plus mosses and short ground cover at the north facing slopes. Collapsed slopes due to permafrost thaw and cryoturbation are also observed in this part of the catchment. Crests

are bare and covered with boulders holding loose aeolian deposits.

### 2.3. DEM preparation

Maps of each site (Figs. 5-9) were made to assign soil profiles to geomorphological units in the landscape (e.g., gentle north facing slope, steep north facing slope). Based on similar studies (e.g., Henkner et al., 2016, Egli et al., 2006 and Temme et al., 2014) the most important landscape features were identified as slope angle, which affects translocation of soil particles, moisture availability and other characteristics (Henkner et al., 2016); aspect, which affects solar radiation (Egli et al., 2006) and can influence aeolian activity and deposition (Goossens, 2006); and curvature, which affects the water holding capacity and flow paths on a smaller scale (Temme et al., 2014). The following decision rules were defined to identify geomorphic characteristics within a landscape:

- Top = highest point, no slope, no aspect
- Crest = convex – convex / convex – straight
- Steep slope > 20°
- Gentle slope > 3° – < 20°
- Valley = concave – straight area between two hills
- Gully = concave – straight area on a slope
- Flat area = no curvature, no aspect, slope < 3°
- Bare rock = steeper than a certain slope depending on parent material
- Aspect = north facing slope between 270 and 90°, south facing slope between 90 and 270°

The Arctic Digital Elevation Models (DEMs) were downloaded from https://www.pgc.umn.edu/data/arcticdem/ (Porter et al., 2018). One tile is 100 km$^2$ and has a resolution of 2x2 m grid cells. The tiles used to cover the study area were combined to one raster using the Mosaic tool in ArcMap. New shape files were created in the catalogue to make a mask of each catchment area and copied to a 32-bit signed raster to be able to add attribute tables and single cell values for further analysis. Catchment boundaries were estimated based on the highest contour lines surrounding the lake and field observations.

Geomorphic characteristics were differentiated by combining conditional statements in the "raster calculator" to assign a true or false statement to raster cells (Fig. 3), resulting in a raster with 1 and 0 values. The tool "set null" was called to assign 'no data' to the cells with a value of 0. To create one new raster of all the 1's for each catchment, another conditional statement was used (con("raster"==1,n + 1,"raster") followed by "mosaic to new raster", which resulted in the maps presented in Figs. 5-9.

### 2.4. Data collection

#### 2.4.1. Field description and classification

Soil profile descriptions were made in the field at stratified points following the WRB classification system and assigned Reference Soil Groups (RSGs) (World Reference Base for Soil Resources, 2006) to understand the spatial variability of soil characteristics with depth. The study sites were visually divided in stratified areas with specific topographies (e.g., ridge, valley, south/north facing slope). Soil pits were dug until bedrock/permafrost was reached or until a depth was reached at which no horizon changes were observed for at least 20 cm.

#### 2.4.2. Soil sample collection and processing

Soil pits forming a catena on the north facing slope of each site were subsampled in 1-cm increments. Additional surface soil samples were collected using a ring corer with a height of 5 cm and a volume of 10 cm$^3$ (n ~ 35 per site). Field notes were made of the coordinates of the sample location, depth (surface 0–5 cm, subsurface 5–10 cm), micro topography (aspect, slope angle, curvature) and vegetation cover. The pH and wetness were measured using an analogue probe (Tecpel pH-707). The scale on the wetness index from 1 = dry to 8 = saturated was strongly affected by the weather conditions prior to measuring and was only used as an indicator for spatial differences.
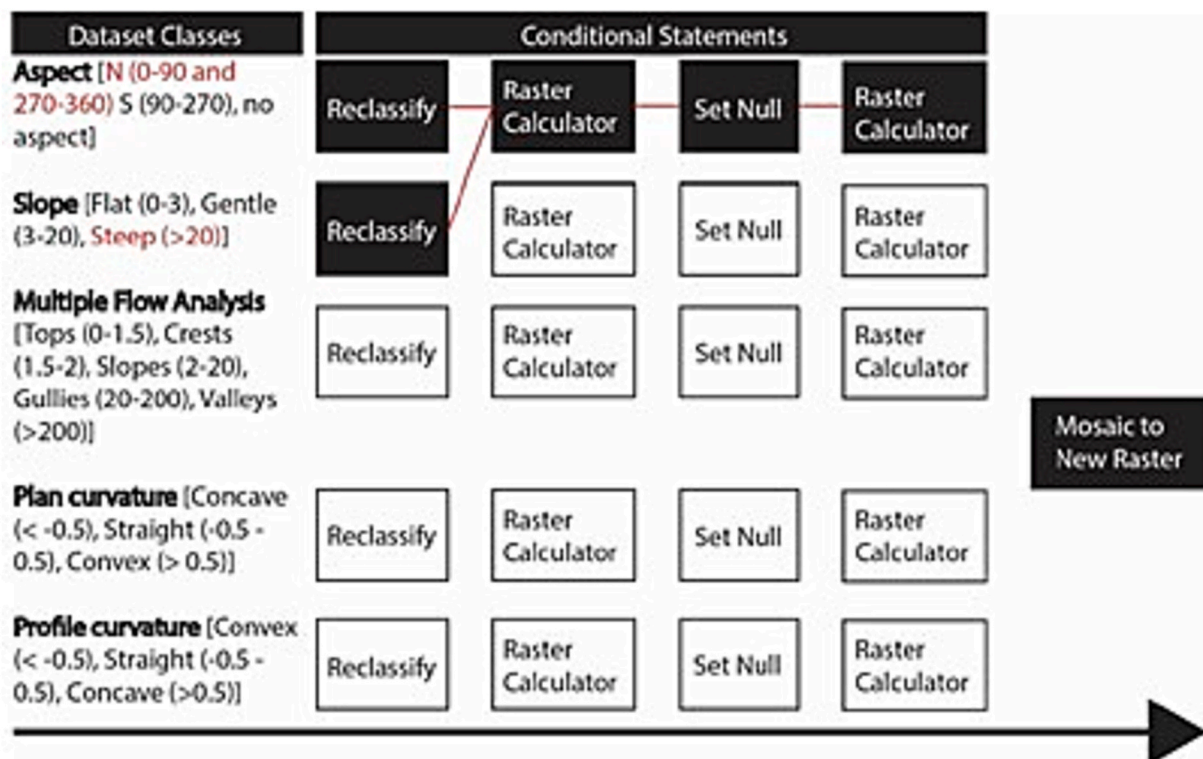


**Fig. 3.** Schematic overview of GIS tools used to assign raster cells to specified geomorphic features.

Samples were dried at 105 °C overnight, passed through a 2 mm sieve to obtain the fine earth fraction and placed in a furnace at 550 °C for 4 h for the loss on ignition of organic matter. A conversion factor of 0.5248 was used to convert the organic matter content into soil organic carbon (SOC) (Parker et al., 2015). Since the amount of elemental C was considered insignificant, the organic C content was equivalent to the total C content (Henkner et al., 2016). Soil bulk density (BD) in $g/cm^3$ was calculated on the fine earth fraction by dividing the weight of the dry soil by the volume. The BD and SOC content of the sub-surface depth increment (5–10 cm) was used to extrapolate the carbon content to depths of 30 cm.

Particle size analysis was conducted on the 1-cm increments using a Beckman Coulter LS 230 laser sizer, giving a volume percentage for 92 size bins ranging from 0.375 – 2000 µm. In the recirculation mode dispersed samples were fully mixed and sampled multiple times being circulated between the vessel and the sample cell with a 67 % pump speed and obscuration rate between 8–12 %. Initial tests were conducted to determine how rapidly the samples dispersed or whether aggregation occurred during the analysis (Mason et al., 2011). Samples were generally stable with minimal disaggregation, so all runs were set to a duration of 60 s and each sample was analysed for 3 runs. This approach quantified particle-sizes of individual particles and transport-stable aggregates. From the full particle-size distributions, all of which were multi-modal, the dominant modes were identified and used to infer possible sediment sources contributing to the soils (Chatenet et al., 1996; Bullard & Austin, 2011).

Fluorescent X-ray energies were measured on the 1-cm increments with an Orbis Edax Ametek micro-XRF. Detectable elements of interest (Al, Ca, Fe, K, Na, Si, Ti) were all measured on the K-line to limit the potential of signal overlap performed under vacuum conditions without filters. Parameter settings were set to 40 keV voltage, 400 µA current, 1.6 µs amplifier time, 30 µm spot size and a 60 s live time. Atmospheric dust samples, collected as described in van Soest et al. (2022), were analysed following the same method.

## 2.5. Spatial and statistical analysis

Spatial modelling techniques were used to extrapolate the point data collected in the field to site and regional scales. Digital Elevation Models (DEM) were used as input data for topographical information of the study area. Relevant summary statistics of the soil characteristics were presented per study site to show the local range in the values obtained. Pearson Correlation Analysis and Multiple/Multivariate Linear regression models were used to explain or predict the amount of SOC for 5 cm and 10 cm soil depth at a given location. The SOC results were linked to DEM derivatives to test the correlation between SOC content and location at the landscape scale using the R software packages *raster* (Hijmans, 2024), *sp* (Pebesma and Bivand, 2005) and *mapview* (Appelhans et al., 2024). The circular aspect radians are converted to Eastness (=Sin(Aspect) with 1 due east and −1 due west) and Northness (=Cos(Aspect) with 1 due north and −1 due south) to create two variables that are linear and therefore more appropriate for analysis. The use of geostatistical kriging and inverse distance weighting were explored as approaches to estimating unknown soil characteristics between known sampling points. However, a uniform distribution of known values is required for an optimal geostatistical fit (Hou et al., 2017) and these approaches did not work effectively for the study sites and are not reported here. Principle Component Analysis was used to identify the directions that maximise variation in the elemental composition of the samples (*stats*, R Core Team, 2013; and *factoextra*, Kassambara and Mundt, 2020 R packages).

## 3. Results

### 3.1. Soil profile descriptions

The most common RSGs described in the area are Regosols, Cambisols, Cryosols and Histosols (Sup. Table S1), for which example profiles are shown in Fig. 4. Buried organic layers are also observed, such as the paleosol in Fig. 4D, and identified with the Thapto subclassifier. Soil depth varied from thin surface layers overlaying bedrock or permafrost to more developed soil profiles consisting of several horizons, including deep C-horizons, reaching total depths of over 80 cm.

Horizon characteristics and layer depths at SS85 are given in Fig. 5. The average profile depth over which soils are observed is 24 cm (standard deviation (σ) ± 2.5 cm). Within the methodological constraints for determining soil depth, soils on the steeper slope positions are shallower than the valley and ridge positions. The active layer depth is constrained by permafrost on the steep north facing slope and in the wetter low-lying areas. Deeper organic horizons are found in these positions as well, with the Ah layer often followed by a second A horizon. Bedrock is reached in all other soil pits apart from Thapto Cambisol (44 cm deep), where the observation depth is based on 'no visible changes' after > 30 cm in what is classified as the C-horizon. Regosols are mainly observed on the crest positions or on the south-facing slopes, whereas slightly more developed Cambisols are found on the north-facing slopes. Histic Cryosols are found on the steep north-facing slopes under layers of moss. Several soil profiles showed signs of paleosols reflecting the strong aeolian history of the area.

The average depth of the soil profiles at SS1590 is 24 cm (σ ± 2.9 cm) (Fig. 6). Within the methodological constraints for determining soil depth, soils on the steeper slope positions are shallower than the valley and ridge positions. Permafrost is visible under the active layer depth on the steep north-facing slope and in the wetter low-lying areas. These soil profiles consisted entirely of organic A(h) horizons and are classified as Histic Cryosols. Soil pits on the steep south facing slope did not have an organic layer at all and are classified as B/C-horizons showing very limited soil development. The most layered soil profiles are found in the gently sloped positions. Regosols are mainly observed on the crest positions or on the south-facing slopes. The water-logged soil in the low land is classified as Muusic Histosol. Several soil profiles showed paleosol characteristics and are classified accordingly.

Horizon characteristics and layer depths at SS17b are given in Fig. 7. The average depth over which soils are observed was 33 cm (σ ± 3.8 cm). In most locations, soils are analysed until bedrock is reached but the soil pits located on the steepest part of the north facing slope are limited in depth due to continuous permafrost and active layer depth of respectively 3 cm and 4 cm. These soils are covered in thick layers of moss (~15 cm). The Cambisol of 64 cm observation depth is based on 'no visible changes' in what is classified as the C-horizon. No visible changes are observed in the B-horizon of the 40-cm Cambisol on the north facing slope, although this deepest soil layer seemed to be very organic and could not be classified as the C-horizon. This profile is described upslope of a ~ 1-m boulder which likely influenced soil formation at that location. Regosols are mainly observed on the crest positions or on the south-facing slopes. Histic cryosols are found on the steep north-facing slopes. Several soil profiles showed paleosol characteristics and are classified accordingly.

The soil pit observations on the Ridge are made along two approximal transects going from uphill to downhill (Fig. 8). Smaller ridges follow the contour lines and create a varied microtopography over the whole study site. The average depth over which soils are observed is 39 cm (σ ± 5.2 cm). Most soils are classified as Cambisol. A relatively thin soil limited by permafrost is observed in a low-lying position of a concave curvature and classified as a Cryosol. The Phaeozem based on the dark colour and organic content is also located in a concave area higher up the Ridge.

The average depth over which soils are observed at SS06 is 40 cm (σ

**A** Profile depth: 14 cm   **B** Profile depth: 24 cm   **C** Profile depth: 40 cm   **D** Profile depth: 37 cm   **E** Profile depth: 34 cm
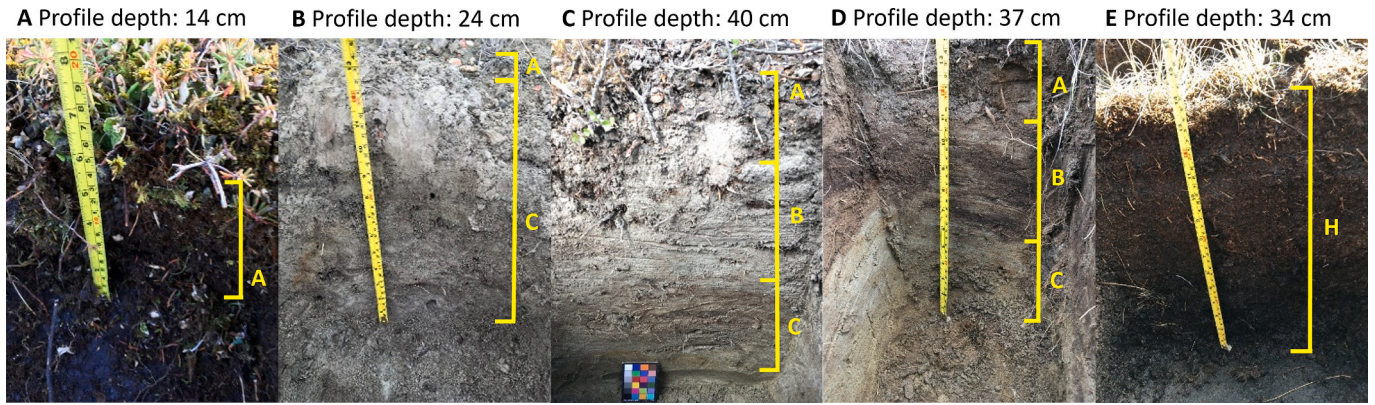


**Fig. 4.** Example pictures of most common soil profiles described in the study area. A) Histic Cryosol, B) Regosol, C) Cambisol, D) Cryosol with paleasol (indicated with Thapto in profile descriptions), and E) Histosol. The total profile depth is given above each picture and the different horizons are indicated with the yellow bar and corresponding letters. (For interpretation of the references to colour in this figure legend, the reader is referred to the web version of this article.)
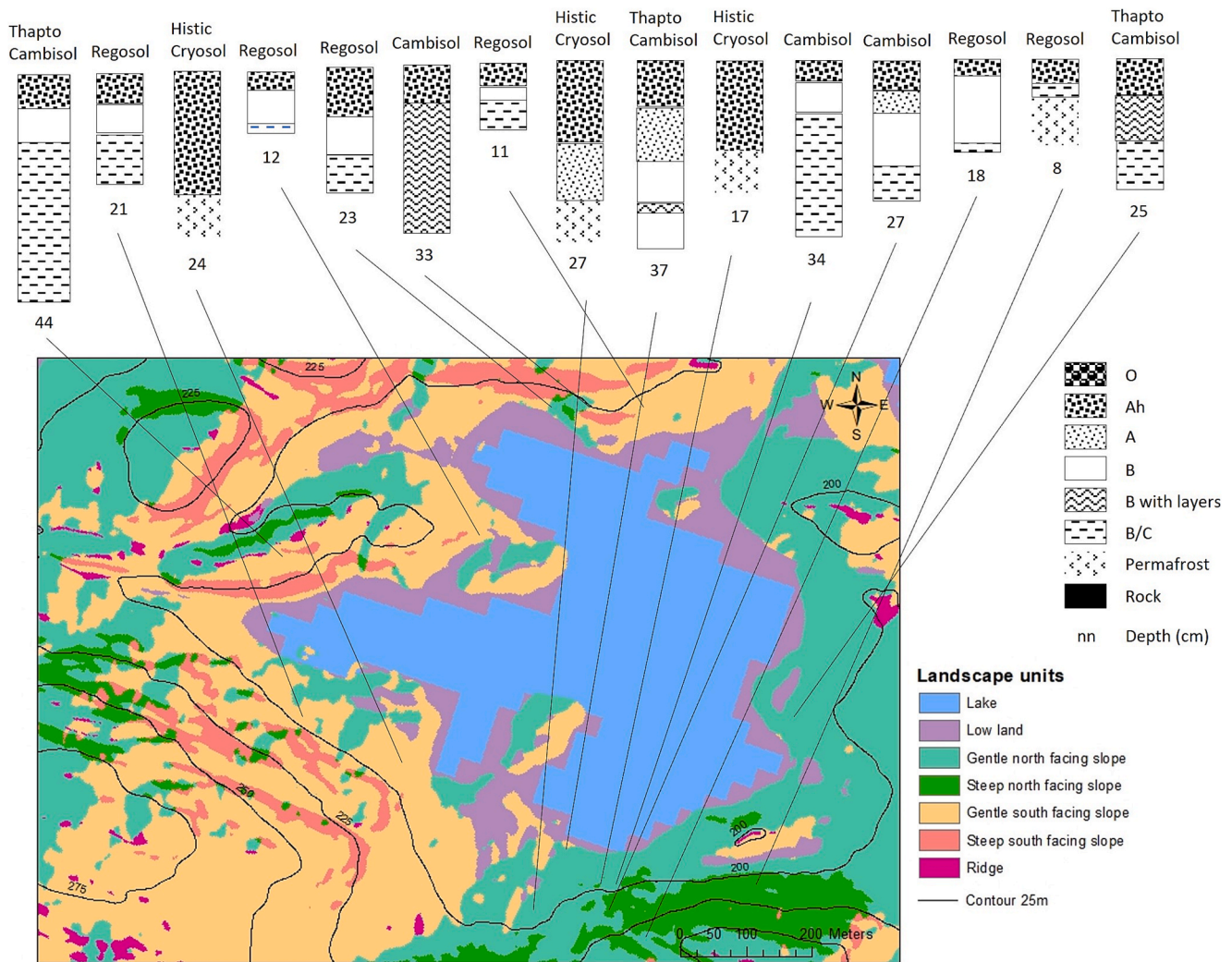


**Fig. 5.** Soil classification SS85. Number at base of each soil profile indicates the depth in cm.

± 4.3 cm) (Fig. 9). Most soils are classified as Cambisols and many of these contained one or more buried organic layers at depth. Regosols are mainly observed on the crest positions and less developed slopes. Two Cryosols are found on the north facing slope, where thawing processes led to the collapse of part of the slope. The water-logged soil in the low land is classified as Muusic Histosol.

### 3.2. Spatial variation in carbon

Correlations at SS85 and SS1590 are mostly negative with the strongest correlation between Eastness (R = −0.35) and the SOC content
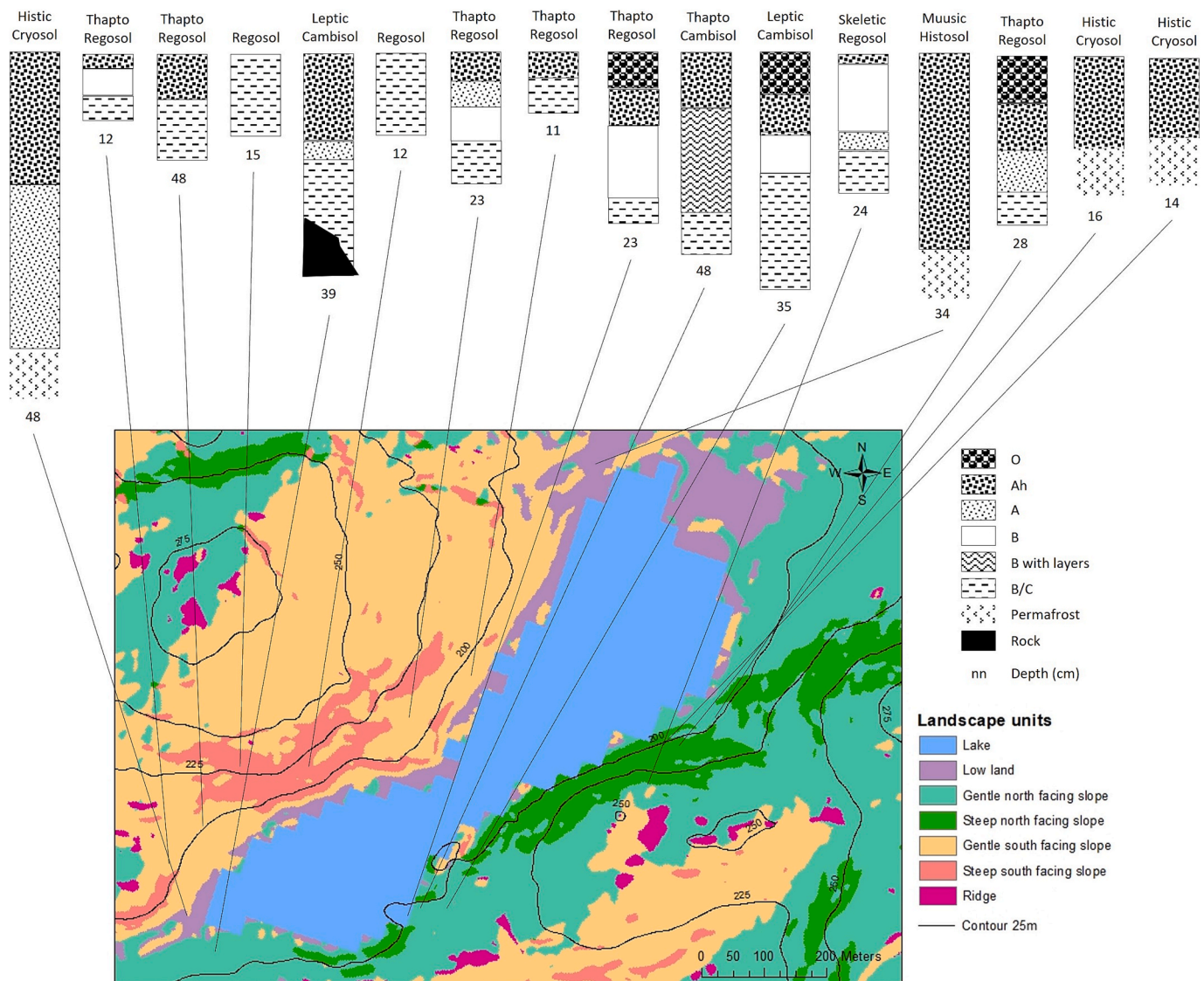
**Fig. 6.** Soil classification SS1590. Number at base of each soil profile indicates the depth in cm.

in the top 5 cm in SS85 and the DEM (R = −0.31) at SS1590 (Table 2). Positive correlations are obtained for SS17b with R = 0.41 for Hillshade and SOC (10 cm). DEM, Flow direction, Hillshade and Northness are positively correlated with SOC content for the Ridge, whereas the correlations with Slope and Eastness are negative. At SS906 the direction of correlations is almost opposite to the Ridge. The SOC content plotted against aspect (Fig. 10) indicates heterogeneous soil carbon storage patterns across the study area. Although north and east facing slopes seem more organic, followed by west facing slopes at SS85, SS17b and SS906, and east facing slopes at SS1590 and the Ridge. Correlations between the SOC content and Pairwise observations did not result in strong or significant correlations, making it statistically difficult to extrapolate the field observations to wider areas via linear models. The overall model strengths predicting the SOC content in the top 5 cm are $R^2 = 0.31$ (p = 0.09) at SS85, $R^2 = 0.12$ (p = 0.5) at SS1590, $R^2 = 0.15$ (p = 0.56) at SS17b, $R^2 = 0.33$ (p = 0.19) at the Ridge, $R^2 = 0.27$ (p = 0.09) at SS906. For the top 10 cm model strengths are $R^2 = 0.22$ (p = 0.09) at SS85, $R^2 = 0.10$ (p = 0.67) at SS1590, $R^2 = 0.38$ (p = 0.028) at SS17b, $R^2 = 0.43$ (p = 0.05) at the Ridge, $R^2 = 0.13$ (p = 0.56) at SS906.

The soil surface throughout each catchment was analysed for basic physical and chemical characteristics (Table 1). Generally, wetter samples have a slightly lower pH, lower BD, and higher OM content. The

correlation between wetness and pH has a $R^2$ = -0.53 (p < 0.0001). There is no clear increase in SOC (LOI%) with distance from the ice sheet with averages being 5.25 % (σ ± 2.64 %) at SS85, 3.74 % (σ ± 2.14 %) at SS1590, 4.00 % (σ ± 1.95 %) at SS17b, 2.13 % (σ ± 1.05 %) at the Ridge and 2.91 % (σ ± 1.31 %) at SS906.

### 3.3. Comparison of soil and dust particles

All the soil and sediment samples analysed have multi-modal particle size distributions. The modes of the particle size distributions (PSD) of the top 1 cm of the soil are compared to the PSD of the dust sampled in August 2017 (Sup. Fig. S2), as well as additional samples collected from the Sandflugtsdalen and Ørkendalen floodplains (Table 3). Apart from the very finest particle size fraction (< 3 μm), dust-sized particles (3–35 μm) are largely absent from the soil samples.

Fig. 11 A and B show the concentration (in weight %) of different elements (Al, Ca, Fe, K, Si, Ti) in soil and dust respectively with distance from the ice margin. Silicon (Si) consistently has the highest concentrations followed by Al. The other elements appear in lower concentrations but show variability across the transect which may indicate changes in soil properties and mineral composition. A Pearson correlation of the elemental concentrations for each site is included in Sup.
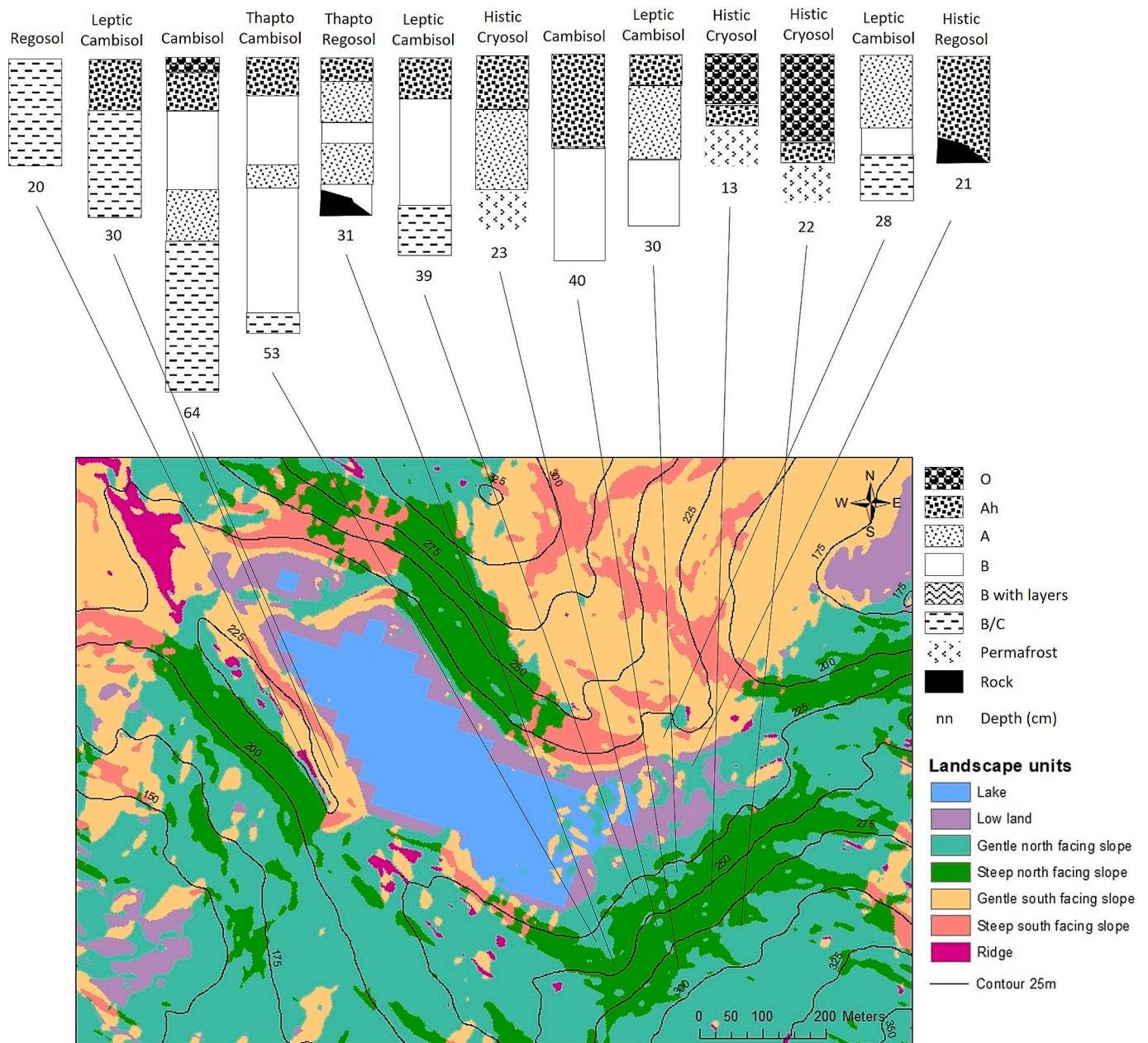
**Fig. 7.** Soil classification SS17b. Number at base of each soil profile indicates the depth in cm.

Table S2. Two principal components can explain 77.1 % of the variance in the dust samples (Fig. 11D) and 69.3 % of the variance in the soil (Fig. 10C). The PCA separated the more organically related elements (Ca, Fe and K) from Al and Si in the dust samples, whereas Al and Ca appear closely related in the soil samples. The higher Ti content in one of the dust samples collected at SS17b pulls this component in an opposite direction of Si in Fig. 11D and F. The individual plots (Fig. 11E and F) show that all sites overlap in elemental composition of the soils, but that the dust is different in SS85. However, the data input for the dust PCA is limited with only two sampling points per site, leading to the individual plot showing a line instead of an ellipse.

## 4. Discussion

### 4.1. Geomorphic and pedogenic processes creating a heterogenous soil landscape

Climate is thought to be a key factor influencing soil development in the Arctic, leading to slow horizon formation and the dominant presence of Cryosols (Gelisols) (Jones et al., 2009), although, at a smaller scale, the soil landscape is heterogenous. Histosols located in wet areas are the result of site-dominated development pathways which means that topography is the dominant factor. In locations where soils are classified as Regosol (Entisol) or Cambisol (Inceptisol), time is the main limiting soil forming factor. To give an estimation of time in cold climate regions, in alpine areas development to Cambisols proceeds within at least 700 years (Dümig et al., 2011).

The wide range in soil types described in the Kangerlussuaq area, and the corresponding degree of soil development, results from the interplay
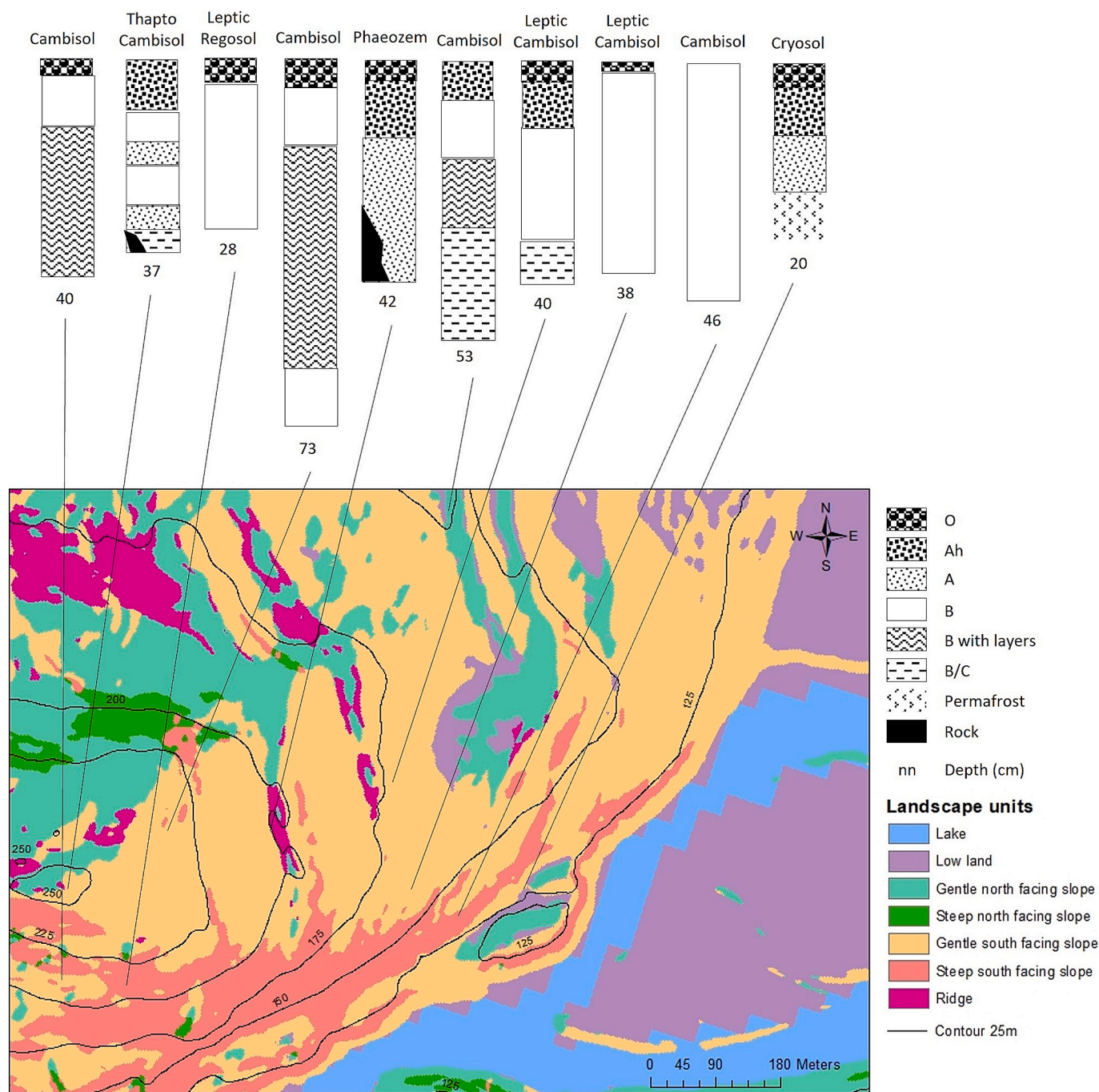
**Fig. 8.** Soil classification Ridge. Number at base of each soil profile indicates the depth in cm.

of multiple soil forming factors. Considering that Stockmann et al (2014) found that soil development rates are in the order of mm kyr$^{-1}$, soils are to be considered young of age. A chrono sequence of soil development, as often found in high altitude paraglacial valleys (e.g. Egli et al., 2006; Temme et al., 2016) or as described in Svalbard (van der Meij et al., 2016) is not visible with distance from the ice sheet in Kangerlussuaq. The gradient in time since deglaciation and onset of soil formation did not have the expected effect on the development stages of soil profiles described within the area. One possible explanation might be that the soil landscape in Kangerlussuaq is analysed across five distinct sites shaped by the retreat of ice sheet outlet glaciers, unlike the single catchment formed by the retreat of a single glacier in the other studies. These geomorphic and spatial differences in slope angles and shape of the terrain influenced the sampling design and could explain the absence

of a clear chrono sequence.

With regards to identifying site-dominated pathways, aspect and altitude are relatively easily identifiable topographic variables in the field or extracted from a DEM. All five study sites have in common that the deeper soils were found in either more stable positions, or on the slopes that receive greater solar radiation. The amount of solar radiation received on a north facing slope at high latitude is substantially less than on a south facing slope, causing differences in light, temperature, moisture and consequently vegetation cover (Egli et al., 2006). Shallow active layers were found on the north-facing slopes, where cooler temperatures limit the seasonal thaw of permafrost. The Regosol in Fig. 4 showed no differentiation in colour or structure, apart from the very thin and dry surface layer and is representative of soils found on south facing slopes. Given the absence of secondary carbonates it is questionable
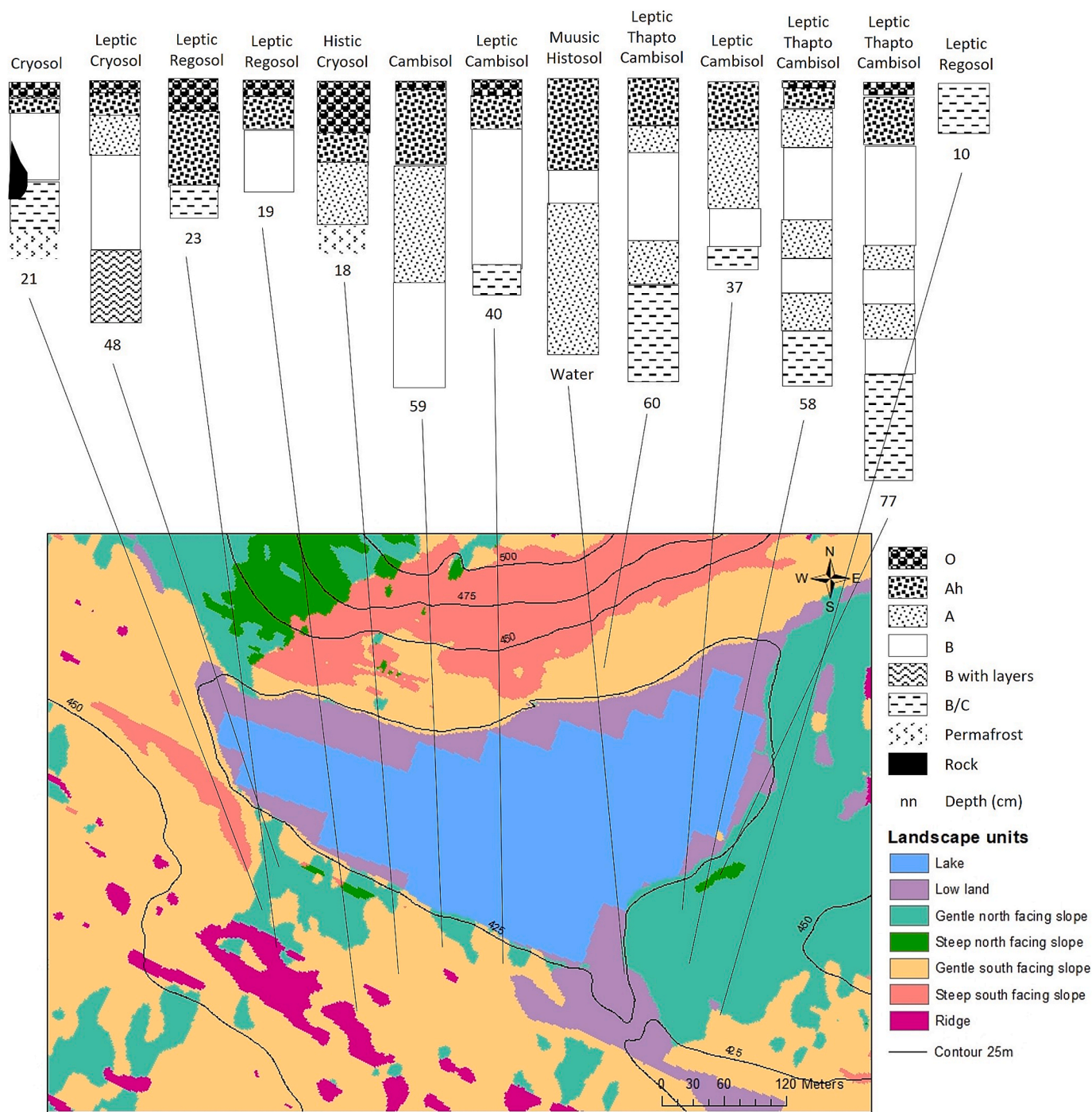
**Fig. 9.** Soil classification SS906. Number at base of each soil profile indicates the depth in cm.

whether there has been any degree of soil formation in profiles that were classified as Regosols. Profiles with active layer depths thinner than 20 cm were also found on the north facing slopes, but their high organic content and visible ice structures indicate a deeper permafrost layer underneath.

This pattern is in agreement with other studies of Arctic soils. For example, the cross sections made by Henkner et al. (2016; Figs. 2-5) show shallower soils on steep north-facing slopes in the Umimmalissuaq valley, West Greenland. They also identified evidence of sediment accumulation on the west-facing slopes, which are situated on the lee-side of the catchments with prevailing eastern winds. Cable et al. (2018) found that on Svalbard drier and deeper active layers on the southern sites of the catchment lack distinct peat layers, whereas the shallower

active layers on the northern sites contained an organic matrix cryo-structure alternating with suspended cryostructure reflecting repeated burial of densely vegetated surfaces. Difference in aspect affects, in addition, patterns of snowpack accumulation and melt, particularly at altitudes with a marginal seasonal snowpack: a persistent snowpack develops on north-facing slopes, whereas snowpack is intermittent on south-facing slopes (Hinckley et al., 2014). The snow cover in Kanger-lussuaq is generally thin (Curtis et al., 2018) and under influence of reworking by wind. Deeper layers of snow were observed to reach up to 50 cm in more sheltered locations during a field season in April 2017, covering most of the vegetation and protecting roots from frost drought. Snow has an insulating effect on soil conditions with warmer soil tem-peratures compared to areas that are snow free (Groffman et al., 2001)

**Table 2**
Correlation between DEM derivatives and SOC content (surface 0–5 and 0–10 cm).

| SS85 | DEM | Slope | Flowdir | Hill | Eastness | Northness | C (5 cm) | C (10 cm) |
|---|---|---|---|---|---|---|---|---|
| DEM | 1.00 | | | | | | | |
| Slope | 0.48 | 1.00 | | | | | | |
| Flowdir | 0.15 | 0.35 | 1.00 | | | | | |
| Hill | 0.27 | 0.06 | 0.43 | 1.00 | | | | |
| Eastness | −0.18 | −0.18 | −0.54 | −0.84 | 1.00 | | | |
| Northness | 0.24 | 0.12 | 0.19 | 0.02 | −0.03 | 1.00 | | |
| C (5 cm) | −0.15 | −0.19 | −0.04 | 0.18 | −0.35 | −0.08 | 1.00 | |
| C (10 cm) | −0.27 | −0.22 | −0.26 | −0.06 | −0.03 | 0.04 | 0.70 | 1.00 |
| **SS1590** | DEM | Slope | Flowdir | Hill | Eastness | Northness | C (5 cm) | C (10 cm) |
| DEM | 1.00 | | | | | | | |
| Slope | 0.49 | 1.00 | | | | | | |
| Flowdir | 0.01 | 0.0.5 | 1.00 | | | | | |
| Hill | −0.02 | −0.07 | 0.51 | 1.00 | | | | |
| Eastness | 0.01 | 0.04 | −0.62 | −0.86 | 1.00 | | | |
| Northness | 0.40 | 0.33 | 0.54 | 0.45 | −0.41 | 1.00 | | |
| C (5 cm) | −0.31 | −0.07 | −0.06 | −0.09 | −0.08 | −0.11 | 1.00 | |
| C (10 cm) | −0.26 | −0.08 | 0.00 | 0.01 | 0.07 | −0.05 | 0.55 | 1.00 |
| **SS17b** | DEM | Slope | Flowdir | Hill | Eastness | Northness | C (5 cm) | C (10 cm) |
| DEM | 1.00 | | | | | | | |
| Slope | 0.60 | 1.00 | | | | | | |
| Flowdir | 0.09 | −0.10 | 1.00 | | | | | |
| Hill | 0.72 | 0.36 | 0.39 | 1.00 | | | | |
| Eastness | −0.58 | −0.25 | 0.55 | −0.87 | 1.00 | | | |
| Northness | 0.25 | 0.06 | 0.18 | 0.12 | −0.11 | 1.00 | | |
| C (5 cm) | 0.15 | 0.04 | 0.14 | 0.23 | −0.10 | 0.05 | 1.00 | |
| C (10 cm) | 0.27 | 0.04 | 0.23 | 0.41 | −0.18 | 0.14 | 0.87 | 1.00 |
| **Ridge** | DEM | Slope | Flowdir | Hill | Eastness | Northness | C (5 cm) | C (10 cm) |
| DEM | 1.00 | | | | | | | |
| Slope | −0.06 | 1.00 | | | | | | |
| Flowdir | −0.13 | −0.33 | 1.00 | | | | | |
| Hill | −0.08 | −0.88 | 0.39 | 1.00 | | | | |
| Eastness | 0.39 | 0.37 | −0.72 | −0.65 | 1.00 | | | |
| Northness | 0.33 | −0.01 | −0.05 | 0.24 | −0.18 | 1.00 | | |
| C (5 cm) | 0.16 | −0.42 | 0.29 | 0.40 | −0.13 | 0.05 | 1.00 | |
| C (10 cm) | 0.17 | −0.40 | 0.44 | 0.44 | −0.27 | 0.15 | 0.90 | 1.00 |
| **SS906** | DEM | Slope | Flowdir | Hill | Eastness | Northness | C (5 cm) | C (10 cm) |
| DEM | 1.00 | | | | | | | |
| Slope | 0.59 | 1.00 | | | | | | |
| Flowdir | 0.11 | −0.06 | 1.00 | | | | | |
| Hill | −0.18 | −0.48 | 0.32 | 1.00 | | | | |
| Eastness | −0.04 | 0.23 | −0.30 | −0.88 | 1.00 | | | |
| Northness | −0.07 | −0.24 | 0.33 | 0.13 | −0.03 | 1.00 | | |
| C (5 cm) | −0.22 | 0.13 | −0.12 | −0.33 | 0.36 | 0.15 | 1.00 | |
| C (10 cm) | −0.13 | 0.01 | 0.12 | −0.03 | 0.07 | 0.28 | 0.61 | 1.00 |

and moreover protects surface particles from erosion.

The sampling location and analysis of soil characteristics were based on a geomorphological approach. By doing so, spatial information on landscape attributes used in the field survey could be included in the mapping process. There are, however, limitations to this approach. Geomorphic maps and soil maps are thematic and often based on those such as the Arctic Digital Elevation Model, making them dependent on the auxiliary material that is available (Miller and Schaetzl, 2016). Another drawback is that for reclassifications arbitrary cut-off values are made based on visual interpretation and expert knowledge (Wielemaker et al., 2001). To validate these cut-off values, a section of the the field data set that was not used for the prediction of the model could be compared to the modelled values by 'Extracting values to points' for those specific coordinates, but one is then still considering the field observations as true values, e.g. the slope angle observed in the field could be compared to the slope angle extracted from the DEM in GIS software. For the geomorphic maps created for this study it is apparent that the north–south divide of the catchments has a strong influence on the slope classification in SS85 and SS906, where parts of the catchment are currently classified as, for example, south facing whilst the real aspect is closer to northeast.

Misrepresentations like these may have been partly avoided by using different conditional statements for each catchment instead of using the same for the entire study area. However, the field observations and sampling design are also based on visual interpretation and expert knowledge. Moreover, Hartemink and Sonneveld (2013) argued that dynamic soil properties such as SOM relate to soil functioning and ecosystem services, whilst soil classification and data collection systems mostly focus on static soil properties. Examples of soil ecosystem services are climate regulation, water purification, nutrient cycling, structural support etc. The field observations used as input for this study are taken from a single sampling scale in time (August 2017) and may have been different in dynamic soil characteristics when measured e.g. a day-, week or year later, although soil characteristics in dry arctic environments are not likely to be that dynamic. In a landscape with a stable geomorphology (no significant erosion or deposition) and deep saturation zone, water flow is essentially vertical and lateral interactions can be ignored, so that representative soil profiles and simulated soil properties can be interpolated (Minasny et al., 2015). A combination of field data collection and simulation modelling is essential to increase the understanding of the soil landscape enabling the researcher to take those ecosystem services into account.

To improve classification accuracy, greater concern should be given to exploring the relationship of topographic parameters to landform shape and spatial extent (Mithan, 2018). Digital soil mapping approaches employ empirical relationships to predict the spatial distribution of soil properties, limited by the observations and the nature of the empirical relationships, and there is a need to use pedological
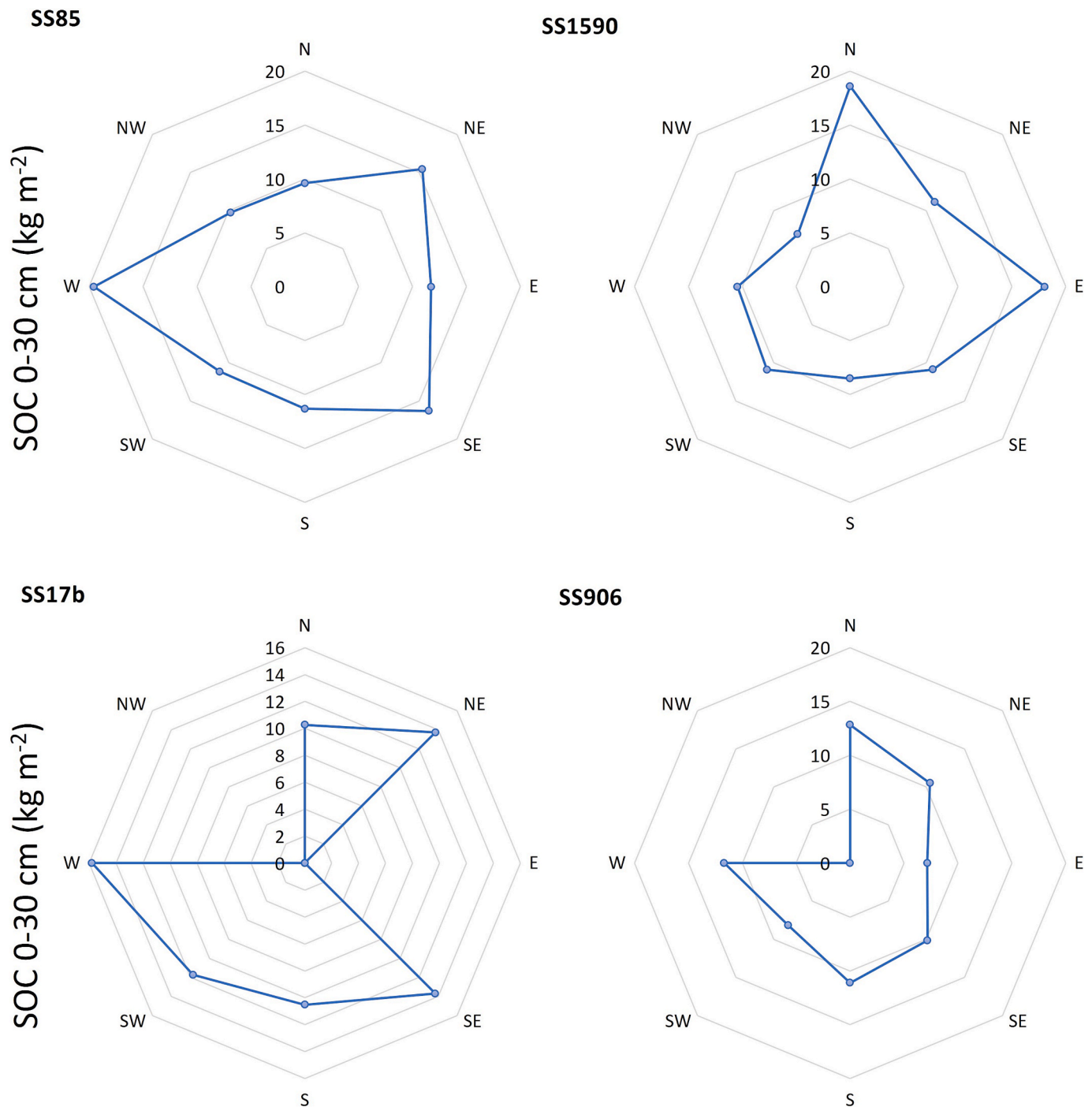
**Fig. 10.** Radar plots representing the distribution of SOC (kg m$^2$) extrapolated to 30 cm depth across aspects for the four lake catchments. Note that the scale describing the SOC at SS17b is different from the other sites.

knowledge to quantitatively relate soil properties to the environmental drivers that form soil (Minasny et al., 2015). Most geostatistical models indirectly predict specific physical or chemical properties of soils incorporating specific spatial uncertainties and are therefore capable of site-specific soil property regionalization but are not process based and do not contribute to the understanding of factor correlations (Bock et al., 2018). It remains difficult to extrapolate the relationships from one catchment to another or wider study region. Although, by incorporating consistent sampling and analysis of the five catchments spread out over the area of interest, the results of this study provide both a better insight into the regional variability and a more reliable input to regional models.

### 4.2. Aeolian deposition and sediment

All soils described in this study are likely to have an aeolian component based on the continuous history of dust deposition within the area after ice retreat. Aeolian processes have been important land-forming factors since deglaciation 8 k yr ago (Storms et al., 2012) and have been continuous over the past 4 k yr (Willemse et al., 2003). It was hypothesised that silt deposited on the floodplain during periods of high meltwater discharge would remain behind as the water recedes, eventually drying out and becoming available for aeolian transport. Dust particles will then be entrained and deposited on the soil surface and materials from all systems expected to have similar particle size

**Table 3**
Particle modes of the soil surface and dust samples.

|  |  | ≈1 µm | 6–10 µm | ≈20 µm | 26–33 µm | 39–84 µm | 111–162 µm | ≈213 µm | 370 – 500 µm | >1000 µm |
|---|---|---|---|---|---|---|---|---|---|---|
| Soil | SS85 | 1.4 |  |  |  | 39.8 | 146.8 |  | 449.7 | 1043 |
|  | SS1590 | 1.3 |  |  |  | 52.6 | 146.8 |  | 493.6 | 1143 |
|  | SS17b | 1.3 |  |  |  | 63.4 |  |  | 493.6 |  |
|  | Ridge | 2.7 |  |  |  | 76.4 | 161.2 |  | 493.6 | 1512 |
|  | SS906 | 1.3 |  |  |  | 63.4 | 161.2 |  | 409.6 | 1143 |
| Dust | SS85 | 1.0 |  | 17.2 | 33.0 |  |  |  |  |  |
|  | SS1590 | 1.0 |  | 17.2 | 33.0 |  |  |  |  |  |
|  | SS17b | 1.0 |  | 15.7 | 30.1 |  |  |  |  |  |
|  | Ridge | 1.3 |  | 20.7 |  |  |  |  |  |  |
|  | SS906 | 0.9 | 6.2 |  | 27.4 | 52.6 | 111.0* |  |  |  |
| Floodplain | D1 | 1.5 |  |  | 33.0 |  | 133.7 |  |  |  |
|  | D2 |  |  |  |  | 39.8 |  |  | 449.7 | 2000 |
|  | D3 | 1.8 |  |  |  |  | 176.9 |  |  | 1377 |
|  | D4 | 1.5 |  |  |  | 43.7 | 133.7 |  |  |  |
|  | D5 | 1.7 |  |  | 27.4 | 83.9 | 161.2 |  | 499.7 | 1143 |
|  | D6 | 1.5 |  |  |  | 52.6 | 146.8 |  | 449.7 |  |
|  | D7 | 1.7 |  |  | 30.1 |  | 161.2 |  | 373.1 |  |
|  | D8 |  |  |  |  |  |  | 213.2 |  |  |
|  | D9 | 1.3 |  |  |  | 43.7 | 133.7 |  |  |  |

*Dust particles are per definition < 63 µm.

distributions. However, since dust typically refers to particles transported in suspension, it is generally limited to those smaller than 63 µm (* in Table 3). Apart from the very finest particle size fraction, dust-sized particles are largely absent from the soil samples. This absence could be attributed to several factors: finer particles may have formed aggregates, become bound to organic matter, broken down further due to in situ weathering, or leached into deeper soil layers. No substantial disaggregation of the particles was observed during analysis. With regards to floodplain samples, timing of collection in August may have meant that most of the dust-sized particles had already been removed from the system by aeolian processes, leaving coarser sediments behind.

Under a dominant wind direction blowing from the ice sheet towards the coast, the aeolian deposits on the west facing (leeward) slopes would be expected to be considerably thicker than the deposits on the east facing slopes (Kidron et al., 2014). Depending on fluctuations in aeolian activity, time since deglaciation may either have resulted in thicker aeolian sediments further away from the GrIS due to the prolonged formation time, or less prominent aeolian dust deposits due to the increasing distance from the active source. The only catchment where the observable depth is the deepest on the west facing slope is SS906, located only 5 km away from the GrIS margin, with the most modern dust deposits and least likely to be affected by multiple sources. This is also the site where the highest average soil depth was observed with 40 cm compared to 24 cm at SS85 located furthest away from the ice sheet, which could indicate that more dust is being deposited at closer to the ice sheet. However, Bullard et al. (2023) found that 10 out of 17 monitored dust events are associated with a westerly wind blowing up-valley towards the ice sheet, indicating a multidirectional wind pattern.

Despite the absence of clear regional trends in dust deposition, the multiple dust sources and multidirectional winds are likely to affect spatial variation in the modern deposits and current degree of soil formation. The ability of soil processes to incorporate the deposits depends both on the amount of material received and the soil forming conditions in which the material is received (Feng et al., 2016). This relationship has implications for both the current influence of dust on the heterogenous soil landscape in Kangerlussuaq with varying soil-moisture regimes related to e.g., aspect and curvature, and on the impact that previous climate fluctuations and aeolian activities will have had on the development of the soil landscape to its current state.

The low-to-the-ground vegetation may also explain why loess deposits are so thin in Kangerlussauq in comparison to other loess regions. Muhs et al. (2004) found a delay in loess sedimentation of ~ 4k years after deglaciation in Alaska and relate this partly to the establishment of boreal forest, which serves as an efficient dust trap compared to herb tundra or even shrub tundra. Less developed near-source soils are described downwind of the Matanuska River in Alaska (Lithosols or Cambisols) and Podzols or Cambisols trending toward Podzols as distal soils, but stratigraphic data also indicated that the complexity of loess sedimentation and pedogenic cycles is at a maximum at intermediate distances from the loess source (Muhs et al. 2004).

### 4.3. Time since deglaciation and spatial variation in soil carbon

Although the exact ages of the described soils are unknown, the ages of the moraines can be used to estimate the time of surface exposure and hence the maximum age of the soils at each of the sites. This would imply that the soils at SS85 and SS1590 are older than the Umivit moraines dated 7.4–7.9cal ka BP and that soils at SS17b located between the Umivit moraine system and Keglen moraines dated at 6.5–7.2cal ka BP started developing some time in between. For the Ridge and SS906 located between the Keglen moraines and current ice sheet margin, it is estimated that the GrIS retreated further inland between ~ 3.4 and ~ 0.5cal ka BP (Willemse et al., 2003) and these catchments have been deglaciated since. However, soils did not appear more substantially developed further away from the ice sheet. Dating of soil profiles, in addition to the already dated moraines, is recommended for future research to better estimate timings in deposition and soil formation.

Soils on north facing slopes appeared much more organic based on the dark colour compared to south facing slopes that were light brown in colour and showed less structure. These field observations are however not reflected in the linear regression models, showing that C content at catchment scale is not significantly linked to topographic landscape variables. On the steeper parts of the north facing slopes, the sampling depths are restricted by active layer depth, whereas these locations are more likely to contain higher organic content stored in frozen soils compared to the deeper mineral soils on south facing slopes. The amount of C, and C loss during or soon after permafrost thaw, in organic-rich soils is thought to depend on permafrost formation processes or the degree of organic matter decomposition that occurs before it is incorporated into what ultimately became permafrost soil horizons (Turetsky et al., 2020).

Topography affects the long-term build-up of OM and ground ice in polar environments, while also influencing thermokarst development and the potential for lateral transport of dissolved and particulate material (Vonk et al., 2019). Pastick et al. (2017) argue that dry aerobic conditions lead to the absence of permafrost, higher rates of decomposition and mineralisation and thin surface organic layers in upland ecosystems, whereas flat, low-lying areas are typically underlain by
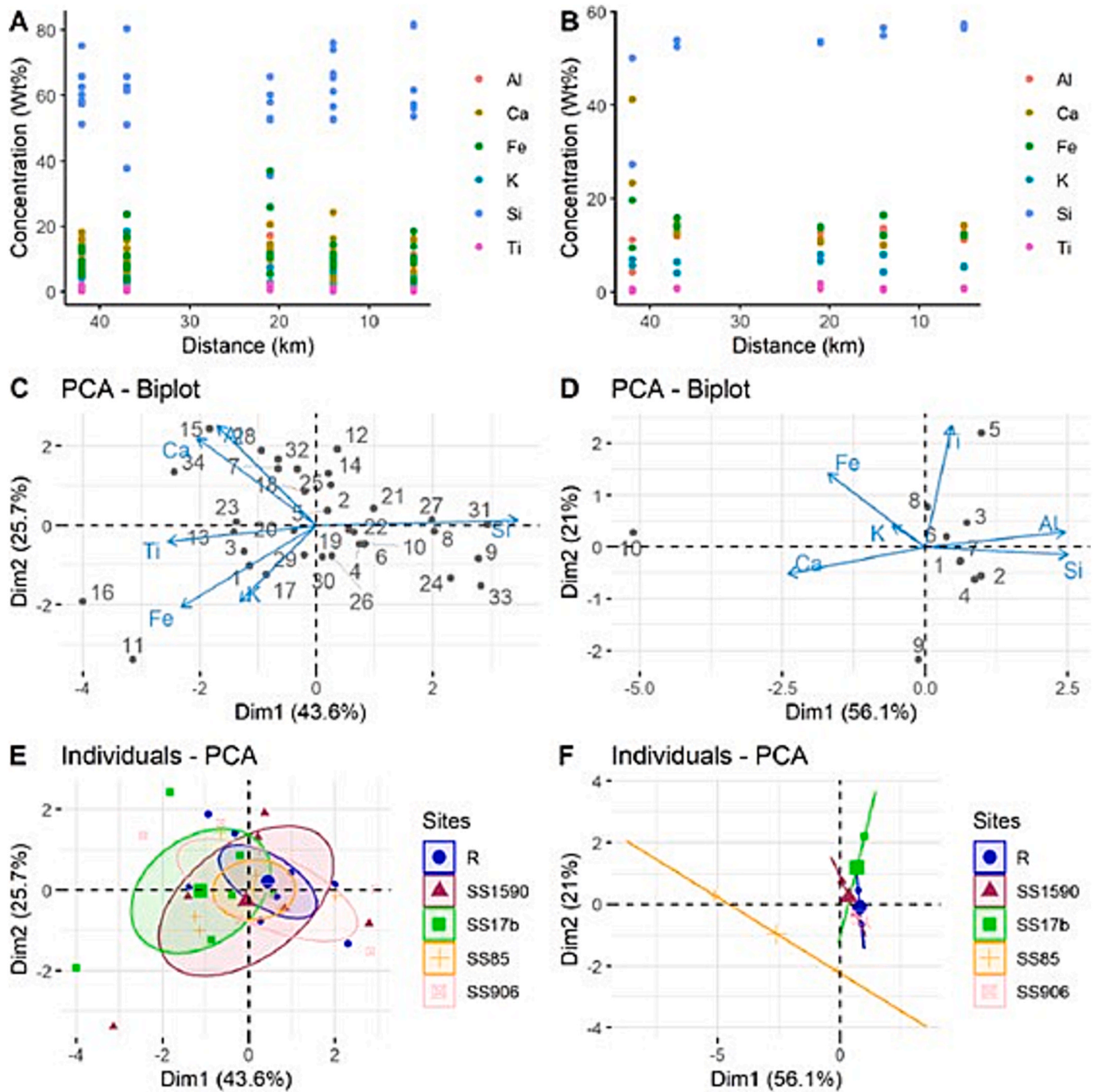
**Fig. 11.** The elemental concentration (Wt%) of soil (A) and dust (B) with distance from the GrIS, Biplots of the principal component analysis show the distribution of the elements (variables) to the components plotted over the soil samples (C) and dust samples (D), and the individual samples are plotted against the PCA axis and grouped per catchment for soil (E) and dust (F). Note: Ellipses could not be drawn for F due to the limited number of samples used. Values on axes differ.

near-surface permafrost leading to perched water tables and anaerobic conditions that slow rates of microbial decomposition and accumulation of large amounts of organic C. These aerobic/anaerobic conditions may be an important reason for the difference described in the presence of OC and permafrost on south and north facing slopes in the Kangerlussuaq area. It also highlights the importance of understanding (changes in) soil hydrology in the dry Arctic of southwest Greenland in addition to wetter parts of the Arctic as these soil environments could respond differently to climate warming.

### 4.4. Direction of future change

Based on permafrost studies elsewhere in Greenland (e.g. Wetterich et al., 2019) and the aeolian history of the landscape (e.g. Willemse, 2003), it is assumed that permafrost in Kangerlussuaq is syngenetic (formed in combination with deposition; Tank et al., 2020) like for example the Yedoma deposits and in contrast to for example the epigenetic permafrost at the Canadian Shield (formed in situ as permafrost base lowers). Given the active layer depth on the south facing slopes is measured to reach the bedrock during the summer, the effect of future permafrost thaw on these parts of the catchments might

be limited, since no major structural disruption is likely to occur. In contrast, on the north facing slope or waterlogged parts of the studied catchments, permafrost thaw and the deepening of the active layer with more ice-rich, mineral- or organic permafrost will release biogeochemical constituents that have been frozen for decades.

## 5. Conclusion

The soil landscape of Kangerlussuaq has been shaped by a complex interplay of geomorphic and environmental processes following the retreat of the Greenland ice sheet. The combination of sediment deposition from glaciers and aeolian sources, in situ physical and chemical weathering, and the translocation of materials through erosion and sedimentation has created a highly heterogeneous soil environment. No significant increase in soil development was found with distance away from the ice sheet. Soil depths vary widely across the landscape, from shallow profiles limited by permafrost or bedrock on steep slopes and crests to deeper, layered soils in gentler or wetter terrain. North-facing slopes and valley positions often have deeper organic horizons, while south-facing slopes show minimal organic layer development. However, correlations between SOC content and landscape variables are weak and site-specific, making it challenging to predict C distribution at broader scales using linear models. These findings provide essential information on how Arctic soils develop, store carbon, and respond to permafrost dynamics. The variability in soil properties across topographic gradients and permafrost-affected areas emphasises the need for fine-scale observations to understand and model Arctic soil systems, particularly in the context of climate change.

## CRediT authorship contribution statement

**Maud A.J. van Soest:** Writing – review & editing, Writing – original draft, Visualization, Validation, Software, Resources, Project administration, Methodology, Investigation, Formal analysis, Data curation, Conceptualization. **N.John Anderson:** Supervision, Funding acquisition, Conceptualization. **Joanna E. Bullard:** Supervision, Funding acquisition, Conceptualization.

## Declaration of competing interest

The authors declare that they have no known competing financial interests or personal relationships that could have appeared to influence the work reported in this paper.

## Acknowledgements

Data availability statement

The data that support the findings of this study are available from the corresponding author upon reasonable request.

## Appendix A. Sup. data

Sup. data to this article can be found online at https://doi.org/10.10 16/j.catena.2025.108938.

## References

Amundson, R., Heimsath, A., Owen, J., Yoo, K., Dietrich, W.E., 2015. Hillslope soils and vegetation. Geomorphology 234, 122–132. https://doi.org/10.1016/j. geomorph.2014.12.031.

Anderson, N.J., Liversidge, A.C., McGowan, S., Jones, M.D., 2012. Lake and catchment response to Holocene environmental change: spatial variability along a climate gradient in southwest Greenland. J. Paleolimnol. 48, 209–222. https://doi.org/10.1007/s10933-012-9616-3.

Anderson, N.J., 2020. Terrestrial ecosystems of West Greenland, in: Encyclopedia of the World's biomes (pp. 551-564). Elsevier. DOI: 10.1016/b978-0-12-409548-9.12486-8.

Anderson, S.P., 2005. Glaciers show direct linkages between erosion rate and chemical weathering fluxes. Geomorphology 67, 147–157. https://doi.org/10.1016/j. geomorph.2004.07.010.

Appelhans, T., Detsch, F., Reudenbach, C., Woelhauer, S. 2024. Mapview: Interactive Viewing of Spatial Data in R. R package version 2.11.2.9000. https://github.com/r-spatial/mapview.

Böcher, T.W., 1949. Racial divergences in Prunella vulgaris in relation to habitat and climate. New Phytol. 48, 289–313.

Bock, M., Conrad, O., Günther, A., Gehrt, E., Baritz, R., Böhner, J., 2018. SaLEM (v1.0) – the Soil and Landscape Evolution Model (SaLEM) for simulation of regolith depth in periglacial environments. Geosci. Model Dev. 11, 1641–1652. https://doi.org/10.5194/gmd-11-1641-2018.

Bosson, J.B., Huss, M., Cauvy-Fraunié, S., Clément, J.C., Costes, G., Fischer, M., Poulenard, J., Arthaud, F., 2023. Future emergence of new ecosystems caused by glacial retreat. Nature 620, 562–569. https://doi.org/10.1038/s41586-023-06302-2.

Bowen, J.C., Ward, C.P., Kling, G.W., Cory, R.M., 2020. Arctic amplification of global warming strengthened by sunlight oxidation of permafrost carbon to $CO_2$. *Geophys. Res. Lett.* 47 (12), e2020GL087085. https://doi.org/10.1029/2020GL087085.

Bullard, J.E., Austin, M.J., 2011. Dust generation on a proglacial floodplain, West Greenland. Aeolian Res. 3, 43–54. https://doi.org/10.1016/j.aeolia.2011.01.002.

Bullard, J.E., Mockford, T., 2018. Seasonal and decadal variability of dust observations in the Kangerlussuaq area, West Greenland. Arct. Antarct. Alp. Res. 50, S100011. https://doi.org/10.1080/15230430.2017.1415854.

Bullard, J.E., Prater, C., Baddock, M.C., Anderson, N.J., 2023. Diurnal and seasonal source-proximal dust concentrations in complex terrain, West Greenland. Earth Surf. Proc. Land. 48 (14), 2808–2827. https://doi.org/10.1002/esp.5661.

Cable, S., Elberling, B., Kroon, A., 2018. Holocene permafrost history and cryostratigraphy in the High-Arctic Adventdalen Valley, central Svalbard. Boreas 47, 423–442. https://doi.org/10.1111/bor.12285.

Chatenet, B., Marticorena, B., Gomes, L., Bergametti, G., 1996. Assessing the microped size distributions of desert soils erodible by wind. Sedimentology 43, 901–911. https://doi.org/10.1111/j.1365-3091.1996.tb01509.x.

Curtis, C.J., Kaiser, J., Marca, A., Anderson, N.J., Simpson, G., Jones, V., Whiteford, E., 2018. Spatial variations in snowpack chemistry, isotopic composition of $NO_3$ and nitrogen deposition from the ice sheet margin to the coast of western Greenland. Biogeosciences 15 (2), 529–550. https://doi.org/10.5194/bg-15-529-2018.

Dijkmans, J.W.A., Törnqvist, T.E., 1991. Modern periglacial eolian deposits and landforms in the Søndre Strømfjord area, West Greenland and their palaeoenvironmental implications. Meddr Grønland, Geosci. 25, 39.

Doetterl, S., Alexander, J., Fior, S., Frossard, A., Magnabosco, C., van de Broek, M., Westergaard, K.B., 2022. J. Plant Nutr. Soil Sci. 185 (1), 19–23. https://doi.org/10.1002/jpln.20210034.

Drohan, P.J., Raab, T., Hirsch, F., 2020. Distribution of silty mantles in soils of the Northcentral Appalachians, USA. Catena 194, 104701. https://doi.org/10.1016/j.catena.2020.104701.

Dümig, A., Smittenberg, R., Kögel-knabner, I., 2011. Concurrent evolution of organic and mineral components during initial soil development after retreat of the Damma glacier, Switzerland. Geoderma 163, 83–94. https://doi.org/10.1016/j. geoderma.2011.04.006.

Egli, M., Hunt, A.G., Dahms, D., Raab, G., Derungs, C., Raimondi, S., Yu, F., 2018. Prediction of Soil Formation as a function of age using the percolation theory approach. Front. Environ. Sci. 6, 108. https://doi.org/10.3389/fenvs.2018.00108.

Egli, M., Mirabella, A., Sartoni, G., Zanelli, R., Bischof, S., 2006. Effect of north and south exposure on weathering rates and clay mineral formation in Alpine soils. Catena 67, 155–174. https://doi.org/10.1016/j.catena.2006.02.010.

Eichel, J., Krautblatter, M., Schmidtlein, S., Dikau, R., 2013. Biogeomorphic interactions in the Trutmann glacier forefield, Switzerland. Geomorphology 201, 98–110. https://doi.org/10.1016/j.geomorph.2013.06.012.

Eichel, J., Corenblit, D., Dikau, R., 2016. Conditions for feedbacks between geomorphic and vegetation dynamics on lateral moraine slopes: a biogeomorphic feedback window. Earth Surf. Process. Landforms 41, 406–419. https://doi.org/10.1002/esp.3859.

Eisner, W.R., Törnqvist, T.E., Koster, E.A., Bennike, O., van Leeuwen, J.F.N., 1995. Paleoecological studies of a Holocene lacustrine record from the Kangerlussuaq (Søndre Strømfjord) region of West Greenland. Quat. Res. 43, 55–66. https://doi.org/10.1006/qres.1995.1006.

Feng, J.-L., Hu, H.-P., Chen, F., 2016. An eolian deposit-buried soil sequence in an alpine soil on the northern Tibetan Plateau: Implications for climate change and carbon sequestration. Geoderma 266, 14–24. https://doi.org/10.1016/j. geoderma.2015.12.005.

Fowler, R.A., Saros, J.E., Osburn, C.L. 2018. Shifting DOC concentration and quality in the freshwater lakes of the Kangerlussuaq region: An experimental assessment of possible mechanisms. Arctic, Antarctic, and Alpine Research 50(1), S100013.

Goossens, D., 1996. Wind tunnel experiments of aeolian dust deposition along ranges of hills. Earth Surf. Process. Landforms. 21 (3), 205–216. https://doi.org/10.1002/(SICI)1096-9837(199603)21:3<205::AID-ESP505>3.0.CO;2-T.

Goossens, D., 2006. Aeolian deposition of dust over hills: the effect of dust grain size on the deposition pattern. Earth Surf. Process. Landforms. 31, 762–776. https://doi.org/10.1002/esp.1272.

Groffman, P.M., Driscoll, C.T., Fahey, T.J., Hardy, J.P., Fitzhugh, R.D., Tierney, G.L., 2001. Colder soils in a warmer world: A snow manipulation study in a northern hardwood forest ecosystem. Biogeochemistry 56, 135–150. https://doi.org/10.1023/A:1013039830323.

Hartemink, A.E., Sonneveld, M.P.W., 2013. Soil maps of the Netherlands. Geoderma 204, 1–9. https://doi.org/10.1016/j.geoderma.2013.03.022.

Heindel, R.C., Chipman, J.W., Virginia, R.A., 2015. The spatial distribution and ecological impacts of aeolian soil erosion in Kangerlussuaq, West Greenland. Ann. Assoc. Am. Geogr. 105, 875–890. https://doi.org/10.1080/00045608.2015.1059176.

Henkner, J., Scholten, T., Kühn, P., 2016. Soil organic carbon stocks in permafrost-affected soils in West Greenland. Geoderma 282, 147–159. https://doi.org/10.1016/j.geoderma.2016.06.021.

Hijmans, R., 2024. Raster: Geographic Data Analysis and Modeling. R package version 3.6-30, https://rspatial.org/raster.

Hinckley, E.-L.-S., Ebel, B.A., Bames, R.T., Anderson, R.S., Williams, M.W., Anderson, S. P., 2014. Aspect control of water movement on hillslopes near the rain snow transition of the Colorado Front Range. Hydrol. Process. 28, 74–85. https://doi.org/10.1002/hyp.9549.

Hobbie, S.E., Nadelhoffer, K.J., Högberg, P., 2002. A synthesis: The role of nutrients as constraints on carbon balances in boreal and arctic regions. Plant and Soil 242, 163–170. https://doi.org/10.1023/A:1019670731128.

Hodkinson, I.D., Coulson, S.J., Webb, N.R., 2003. Community assembly along proglacial chronosequences in the high Arctic: vegetation and soil development in north-west Svalbard. J. Ecol. 91 (4), 651–663. https://www.jstor.org/stable/3599578.

Hou, D., O'Connor, D., Nathanial, P., Tian, L., Ma, Y., 2017. Integrated GIS and multivariate statistical analysis for regional scale assessment of heavy metal soil contamination: A critical review. Environ. Pollut. 231, 1188–1200. https://doi.org/10.1016/j.envpol.2017.07.021.

Hugelius, G., Tarnocai, C., Broll, G., Canadell, J.G., Kuhry, P., Swanson, D.K., 2013. The Northern Circumpolar Soil Carbon Database: spatially distributed datasets of soil coverage and soil carbon storage in the northern permafrost regions. Earth Syst. Sci. Data 5 (1), 3–13. https://doi.org/10.5194/essd-5-3-2013.

Jenny, H., 1941. Factors of soil formation. McGraw-Hill Book Co., New York.

Jones, A., Stolbovoy, V., Tarnocai, C., Broll, G., Spaargaren, O., Montanarella, L. (Eds.), 2009. Soil Atlas of the Northern Circumpolar Region. European Commission Office for Official Publications of the European Communities, Luxembourg, p. 142.

Kassambara, A., Mundt, F., 2020. Factoextra: Extract and Visualize the Results of Multivariate Data Analyses. R Package Version 1, 7. https://CRAN.R-project.org/package=factoextra.

Kidron, G.J., Zohar, M., Starinsky, A., 2014. Spatial distribution of dust deposition within a small drainage basin: implications for loess deposits in the Negev Desert. Sedimentology 61, 1908–1922. https://doi.org/10.1111/sed.12121.

Lawrence, C.R., Schulz, M.S., Masiello, C.A., Chadwick, O.A., Harden, J.W., 2021. The trajectory of soil development and its relationship to soil carbon dynamics. Geoderma 403, 115378. https://doi.org/10.1016/j.geoderma.2021.115378.

Lev, A., King, R.H., 1999. Spatial variation of soil development in a high arctic soil landscape: Truelove Lowland, Devon Island, Nunavut. Canada. Permafrost and Periglacial Processes. 10, 289–307. https://doi.org/10.1002/(SICI)1099-1530(199907/09)10:3<289::AID-PPP319>3.0.CO;2-Z.

Mason, J.A., Nater, E.A., Zanner, C.W., Bell, J.C., 1999. A new model of topography effects on the distribution of loess. Geomorphology 28 (3–4), 223–236. https://doi.org/10.1016/S0169-555X(98)00112-3.

Mason, J.A., Greene, R.S.B., Joeckel, R.M., 2011. Laser diffraction analysis of the disintegration of Aeolian sedimentary aggregates in water. Catena 87, 107–118. https://doi.org/10.1016/j.catena.2011.05.015.

Meier, L.A., Krauze, P., Prater, I., Horn, F., Schaefer, C.E., Scholten, T., Wagner, D., Mueller, C.W., Kühn, P., 2019. Pedogenic and microbial interrelation in initial soils under semiarid climate on James Ross Island, Antarctic Peninsula region. Biogeosciences 16, 2481–2499. https://doi.org/10.5194/bg-16-2481-2019.

Miller, B.A., Schaetzl, R.J., 2016. History of soil geography in the context of scale. Geoderma 264, 284–300. https://doi.org/10.1016/j.geoderma.2015.08.041.

Milne, G., 1935. Some suggested units of classification and mapping for East African soils. Soil Res. 4, 183–198.

Minasny, B., Finke, P., Stockmann, U., Vanwallegham, T., McBratney, A.B., 2015. Resolving the integral connection between pedogenesis and landscape evolution. Earth Sci. Rev. 150, 102–120. https://doi.org/10.1016/j.earscirev.2015.07.004.

Mithan, H.T., 2018. Quantifying the dynamic response of permafrost and slope stability to a changing climate. School of Earth and Ocean Sciences Cardiff University. https://orca.cardiff.ac.uk/id/eprint/111329.

Muhs, D.R., 2013. The geologic record of dust in the Quaternary. Aeolian Res. 9, 3–48. https://doi.org/10.1016/j.aeolia.2012.08.001.

Muhs, D.R., McGeehin, J.P., Beann, J., Fisher, E., 2004. Holocene loess deposition and soil formation as competing processes, Matanuska Valley, southern Alaska. Quat. Res. 61, 265–276. https://doi.org/10.1016/j.yqres.2004.02.003.

Müller, M., Thiel, C., Kühn, P., 2016. Holocene palaeosols and aeolian activities in the Umimmalissuaq valley, West Greenland. The Holocene 26, 1149–1161. https://doi.org/10.1177/0959683616632885.

Ozols, U., Brol, G., 2005. Soil Ecological processes in vegetation patches of well drained permafrost affected sites (Kangerlussuaq-West Greenland). Polarforschung 73, 5–14.

Parker, T.C., Subke, J.-A., Wookey, P.A., 2015. Rapid carbon turnover beneath shrub and tree vegetation is associated with low soil carbon stocks at a subarctic treeline. Glob. Chang. Biol. 21, 2070–2081. https://doi.org/10.1111/gcb.12793.

Pastick, N.J., Duffy, P., Genet, H., Rupp, T.S., Wylie, B.K., Johnson, K.D., Jorgenson, M. T., Bliss, N., McGuire, A.D., Jafarov, E.E., Knight, J.F., 2017. Historical and projected trends in landscape drivers affecting carbon dynamics in Alaska. Ecol. Appl. 27, 1383–1402. https://doi.org/10.1002/eap.1538.

Pebesma, E., Bivand, R., 2005. Classes and methods for spatial data in R. R News 5 (2), 9–13. https://cran.r-project.org/doc/Rnews/.

Petrone, J., Sohlenius, G., Johansson, E., Lindborg, T., Näslund, J.-O., Strömgren, M., Brydsten, L., 2016. Using ground-penetrating radar, topography and classification of vegetation to model the sediment and active layer thickness in a periglacial lake catchment, western Greenland. Earth Syst. Sci. Data. 8, 663–677. https://doi.org/10.5194/essd-8-663-2016.

Phillips, C.A., Elberling, B., Michelsen, A., 2019. Soil Carbon and Nitrogen Stocks and Turnover Following 16 years of Warming and Litter Addition. Ecosystems 22, 110–124. https://doi.org/10.1007/s10021-018-0256-y.

Porter, C., et al., 2018. "ArcticDEM, Version 3". DOI: 10.7910/DVN/OHHUKH, Harvard Dataverse, V1 (accessed 2018).

R Core Team, 2013. R: A language and environment for statistical computing. R Foundation for Statistical Computing, Vienna, Austria http://www.R-project.org.

Rosenbloom, N.A., Doney, S.C., Schimel, D.S., 2001. Geomorphic evolution of soil texture and organic matter in eroding landscapes. Global Biogeochem. Cycles 15, 365–381. https://doi.org/10.1029/1999GB001251.

Saros, J.E., et al., 2019. Arctic climate shifts drive rapid ecosystem responses across the West Greenland landscape. Environ. Res. Lett. 14, 074027. https://doi.org/10.1088/1748-9326/ab2928.

Schaphoff, S., Heyder, U., Ostberg, S., Gerten, D., Heinke, J., Lucht, W., 2013. Contribution of permafrost soils to the global carbon budget. Environ. Res. Lett. 8, 014026. https://doi.org/10.1088/1748-9326/8/1/014026.

Sommer, M., Schlichting, E., 1997. Archetypes of catenas in respect to matter – a concept for structuring and grouping catenas. Geoderma 76, 1–33. https://doi.org/10.1016/S0016-7661(96)00095-X.

Stockmann, U., Minasny, B., McBratney, A.B., 2014. How fast does soil grow? *Geoderma* 216, 48–61. https://doi.org/10.1016/j.geoderma.2013.10.007.

Storms, J.E.A., de Winter, I.L., Overeem, I., Drijkoningen, G.G., Lykke-Andersen, H., 2012. The Holocene sedimentary history of the Kangerlussuaq Fjord-valley fill, West Greenland. Quaternary Science Reviews. 1-22. doi:10.10.1016/j.quascirev.2011.12.014.

Schuur, E.A.G., McGuire, A.D., Schädel, C., Grosse, G., Harden, J.W., Hayes, J.W., Hugelius, G., Koven, C.D., Kuhry, P., Lawrence, D.M., Natali, S.M., Olefeldt, D., Romanovsky, V.E., Schaefer, K., Turetsky, M.R., Treat, C.C., Vonk, J.E., 2015. Climate change and the permafrost carbon feedback. Nature 520, 171–179. https://doi.org/10.1038/nature14338.

Tank, S.E., Mcclelland, J.W., Vonk, J.E., Walvoord, M.A., Laurion, I., Abbott, B.W., 2020. Landscape matters: Predicting the biogeochemical effects of permafrost thaw on aquatic networks with a state factor approach. Permafr. Periglac. Process. 31, 358–370. https://doi.org/10.1002/ppp.2057.

Tape, K.D., Verbyla, D., Welker, J.M., 2011. Twentieth century erosion in Arctic Alaska foothills: The influence of shrubs, runoff, and permafrost. J. Geophys. Res. 116, G04024. https://doi.org/10.1029/2008GB003327.

Tarnocai, C., Canadell, J.G., Schuur, E.A., Kuhry, P., Mazhitova, G., Zimov, S., 2009. Soil organic carbon pools in the northern circumpolar permafrost region. Global Biogeochem. Cycles 23 (2). https://doi.org/10.1029/2008GB003327.

Temme, A.J.A.M., Heckmann, T., Harlaar, P., 2016. Silent play in a loud theatre – Dominantly time-dependent soil development in the geomorphically active proglacial area of the Gepatsh glacier. Austria. Catena. 147, 40–50. https://doi.org/10.1016/j.catena.2016.06.042.

Temme, A.J.A.M., Lange, K., 2014. Pro-glacial soil variability and geomorphic activity-the case of three Swiss valleys. Earth Surf. Process. Landforms. 39, 1492–1499. https://doi.org/10.1002/esp.3553.

Turetsky, M.R., Abbott, B.W., Jones, M.C., Walter Anthony, K., Olefeldt, D., Schuur, E.A. G., Grosse, G., Kuhry, P., Hugelius, G., Koven, C., Lawrence, D.M., Gibson, C., Sannel, A.B.K., McGuire, A.D., 2020. Carbon release through abrupt permafrost thaw. Nat. Geosci. 13, 138–143. https://doi.org/10.1038/s41561-019-0526-0.

van der Meij, W.M., Temme, A.J.A.M., de Klein, C.M.F.J.J., Reimann, T., Heuvelink, G.B. M., Zwoliński, Z., Rachlewicz, G., Rymer, K., Sommer, M., 2016. Arctic soil development on a series of marine terraces on central Spitsbergen, Svalbard: a combined geochronology, fieldwork and modelling approach. Soil. 2, 221–240. https://doi.org/10.5194/soil-2-221-2016.

van Soest, M.A.J., Bullard, J.E., Prater, C., Baddock, M.C., Anderson, N.J., 2022. Annual and seasonal variability in high latitude dust deposition, West Greenland. Earth Surf. Proc. Land. 47, 2393–2409. https://doi.org/10.1002/esp.5384.

van Tatenhove, F.G.M., Olesen, O.B., 1994. Ground temperature and related permafrost characteristics in West Greenland. Permafr. Periglac. Process. 5, 199–215. https://doi.org/10.1002/ppp.3430050402.

van Tatenhove, F.G.M., Fabre, A., Greve, R., Huybrechts, P., 1996. Modelled ice-sheet margins of three Greenland ice-sheet models compared with a geological record from ice-marginal deposits in central West Greenland. Ann. Glaciol. 23, 52–58. https://doi.org/10.3189/S0260305500013252.

Vonk, J.E., Tank, S.E., Walvoord, M.A., 2019. Integrating hydrology and biogeochemistry across frozen landscapes. Nat. Commun. 10, 5377. https://doi.org/10.1038/s41467-019-13361-5.

Wallroth, T., Lokrantz, H., Ritsma, A., 2010. The Greenland Analogue Project (GAP). Literature review of hydrogeology/hydrogeochemistry (No. SKB-R-10-34). Swedish Nuclear Fuel and Waste Management Co.

Wetterich, S., Davidson, T.A., Bobrov, A.A., Opel, T., Windirsch, T., Johansen, K.L., González-Bergonzoni, I., Mosbech, A., Jeppesen, E., 2019. Stable isotope signatures of Holocene syngenetic permafrost trace seabird presence in the Thule District (NW Greenland). Biogeoscience Discussions 1–25. https://doi.org/10.5194/bg-2019-71.

Wielemaker, W.G., de Bruin, S., Epema, G.F., Veldkamp, A., 2001. Significance and application of the multi-hierarchical landsystem in soil mapping. Catena 43, 15–34. https://doi.org/10.1016/S0341-8162(00)00121-1.

Willemse, N.W., Koster, E.A., Hoogakker, B., van Tatenhove, F.G.M., 2003. A continuous record of Holocene eolian activity in West Greenland. Quat. Res. 59, 322–334. https://doi.org/10.1016/S0033-5894(03)00037-1.

Winsor, K., Carlson, A.E., Caffee, M.W., Rood, D.H., 2015. Rapid last-deglacial thinning and retreat of the marine-terminating southwestern Greenland ice sheet. Earth Planet. Sci. Lett. 426, 1–12. https://doi.org/10.1016/j.epsl.2015.05.040.

Wojcik, R., Eichel, J., Bradley, J.A., Benning, L.G., 2021. How allogenic factors affect succession in glacier forefields. Earth Sci. Rev. 218, 103642. https://doi.org/10.1016/j.earscirev.2021.103642.

Young, N.E., Briner, J.P., 2015. Holocene evolution of the western Greenland Ice Sheet: Assessing geophysical ice-sheet models with geological reconstructions of ice-margin change. Quat. Sci. Rev. 114, 1–17. https://doi.org/10.1016/j.quascirev.2015.01.018.